J. Fluid Mech. (1991), *vol.* 228, *pp.* 561–606
Printed in Great Britain

Quenching processes and premixed turbulent combustion diagrams

By T. POINSOT[1,2]†, D. VEYNANTE[2] AND S. CANDEL[2]

[1] Center for Turbulence Research, Stanford University, Stanford, CA 94305, USA

[2] Laboratoire EM2C, CNRS, Ecole Centrale de Paris, 92295 Chatenay-Malabry Cedex, France

(Received 13 March 1990 and in revised form 15 January 1991)

The structure of premixed turbulent flames is a problem of fundamental interest in combustion theory. Possible flame geometries have been imagined and diagrams indicating the corresponding regimes of combustion have been constructed on the basis of essentially intuitive and dimensional considerations. A new approach to this problem is described in the present paper. An extended definition of flamelet regimes based on the existence of a continuous active (not quenched) flame front separating fresh gases and burnt products is first introduced. Direct numerical simulations of flame/vortex interactions using the full Navier–Stokes equations and a simplified chemistry model are then performed to predict flame quenching by isolated vortices. The formulation includes non-unity Lewis number, non-constant viscosity and heat losses so that the effect of stretch, curvature, transient dynamics and viscous dissipation can be accounted for. As a result, flame quenching by vortices (which is one of the key processes in premixed turbulent combustion) may be computed accurately. The effects of curvature and viscous dissipation on flame/vortex interactions may also be characterized by the same simulations. The influence of non-unity Lewis number and of thermo-diffusive processes in turbulent premixed combustion is discussed by comparing flame responses for two values of the Lewis number ($Le = 0.8$ and 1.2). An elementary ('spectral') diagram giving the response of one flame to a vortex pair is constructed. This spectral diagram is then used, along with certain assumptions, to establish a turbulent combustion diagram similar to those proposed by Borghi (1985) or Williams (1985). Results show that flame fronts are much more resistant to quenching by vortices than expected from the classical theories. A cut-off scale and a quenching scale are also obtained and compared with the characteristic scales proposed by Peters (1986). Results show that strain is not the only important parameters determining flame/vortex interaction. Heat losses, curvature, viscous dissipation and transient dynamics have significant effects, especially for small scales and they strongly influence the boundaries of the combustion regimes. It is found, for example, that the Klimov–Williams criterion which is generally advocated to limit the flamelet region, underestimates the size of this region by more than an order of magnitude.

1. Introduction

While premixed turbulent combustion is of considerable technological interest, its modelling is still largely based on empirical ideas. This is due to the complexity of flame/turbulence interactions. An important aspect in the derivation of a turbulent

† Author to whom correspondence should be addressed, at the Ecole Centrale de Paris.

combustion model is to determine the combustion regime and the structure of the reacting flow. Diagrams defining combustion regimes in terms of length and velocity-scale ratios have been proposed by Barrère (1974), Bray (1980), Borghi (1985, 1988), Peters (1986), Williams (1985) and Abdel-Gayed & Bradley (1985, 1989). Knowing the integral turbulence scale and the turbulent kinetic energy, these diagrams indicate whether the flow will feature flamelets, pockets or distributed reaction zones. The dimensional arguments which are used to derive these diagrams are mainly intuitive and leave aside important phenomena such as flame front curvature, dynamical features or viscous effects. This article proposes a new method leading to a classification which accounts for these effects. It mainly focuses on the problems of flame quenching by turbulence which constitutes one important mechanism in many models of premixed turbulent combustion as well as in the construction of the corresponding diagrams (Borghi 1985, 1988).

Flame quenching occurs when a flame front is submitted to external perturbations like heat losses or aerodynamic stretch which are sufficiently strong to decrease the reaction rate through the flame front to a negligible value or in some cases to completely suppress the combustion process. For example, asymptotic studies of laminar stagnation-point flames established by the counterflow of reactants and products (Bush & Fendell 1970; Libby & Williams 1982; Libby, Liñàn & Williams 1983) reveal that stretch may significantly decrease the flame speed. Libby *et al.* (1983) show that quenching by stretch may occur if the flow is non-adiabatic or if the Lewis number (defined as the ratio of the thermal diffusivity to the reactant diffusivity: $Le = \lambda/(\rho C_p \mathscr{D})$) is greater than unity. These results are confirmed for simple or complex chemistry, by numerical calculations (for example, Darabiha, Candel & Marble 1986; Giovangigli & Smooke 1987) and experimental studies (Ishizuka & Law 1982; Sato 1982; Law, Zhu & Lu 1986). Figure 1 gives a graphic summary of the effects of stretch on the flame speed of a laminar flame front with and without heat losses. The idea that such mechanisms may be responsible for partial or total quenching in premixed turbulent flames is an important ingredient of many models (Peters 1986; Bray 1987; Darabiha *et al.* 1989; Candel *et al.* 1990).

At this point, it is important to discuss the definition of the flamelet regime. Depending on the type of model which one wishes to apply, one may use two alternative definitions of the flamelet regime of combustion.

(i) The first approach, which we will call the *laminar flamelet* (*LF*) *assumption* is based on two hypotheses. The first is related to the topology of the flow. It basically requires that the reacting flow may be viewed as a two-fluid flow: the fresh and the burnt gases, separated by an interface (the flame surface) where chemical reactions take place. In this regime, fresh and hot gases burn before they can diffuse and mix. In this sense, the flamelet assumption is equivalent to the classical 'fast chemistry' assumption. Modelling turbulent premixed combustion under the flamelet assumption reduces the general problem of turbulent combustion to the description of the flame surface. This characterization includes two aspects: the total area of the flame surface and the local consumption rate along the flame surface. The second hypothesis in the LF approach is related to the structure of the flame front. This interface between fresh and burnt gases is assumed to behave exactly like a small laminar flame (a 'flamelet'). If flamelets are also assumed to be planar and steady, the local consumption rate is then simply equal to the consumption rate of a steady planar laminar flame so that only the flame front area needs to be modelled. Note that tracking the area of the flame surface (Marble & Broadwell 1977; Candel *et al.* 1990; Darabiha *et al.* 1989; Pope & Cheng 1988) is essentially equivalent to tracking

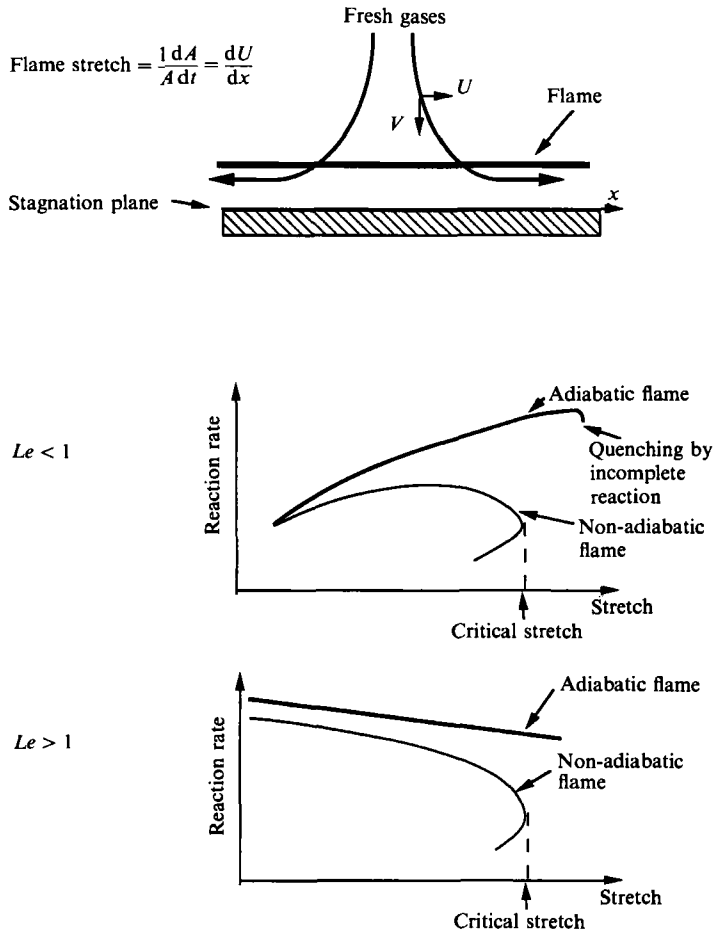

FIGURE 1. The effect of flame stretch on laminar flames at stagnation point (Libby *et al.* 1983).

the passage frequency of the flamelets (Bray & Libby 1986; Cant & Bray 1988; Cheng, Shepherd & Talbot 1988).

(ii) The second approach, which we will call the *extended flamelet* (*EF*) *assumption* is less restrictive than the laminar flamelet (LF) assumption. It uses only the first hypothesis of the LF assumption: the flow is assumed to feature fresh and burnt gases separated by an interface but this interface may not have an exactly laminar structure so that the local consumption rate is not directly related to a laminar situation. Indeed, recent direct simulations show that the local consumption rate is a quantity which changes in smaller proportions than the flame surface (Ashurst, Peters & Smooke 1987; Rutland & Trouvé 1990; Haworth & Poinsot 1990) so that its precise determination is probably less critical than a knowledge of the flame surface.

Discussing the merits of each of these assumptions in terms of turbulent combustion models is beyond the scope of this paper. As pointed out by R. Borghi (private communication), the laminar flamelet assumption (LF) is the easiest to use because it allows a determination of the local consumption rate using standard laminar flame models whose characteristics may be stored in flamelet libraries (Bray 1987; Candel *et al.* 1990; Cant & Bray 1988). However, because of its numerous hypotheses (steady, planar, laminar-like flamelets), the laminar flame assumption is

rarely rigorously satisfied and it is believed that it limits the applicability of flamelet models by imposing too strong constraints. Many authors already indicate that in order to compare turbulent flamelets and laminar flames, stretch (Williams 1985) but also curvature (Mikolaitis 1984*a*, *b*; Haworth & Poinsot 1990; Rutland & Trouvé 1990; Cant & Rutland 1990) and unsteady effects (Haworth *et al.* 1988) have to be included in the laminar situations. Our own feeling is that the important assumption in flamelet modelling is related to the topology of the flow and to the fact that fresh and burnt gases are separated by a relatively thin region with a recognizable structure in which the chemical reactions proceed to completion. This property alone reduces the modelling of turbulent combustion to a more tractable two-fluid problem (fresh and burnt gases) which may be attacked with statistical tools. The flame front separating the fresh and burnt gases may have a laminar structure as required in the LF approach but this is not necessary to construct an operational combustion model. The simulations carried out in this article indicate that the flame surface may be submitted to curvature, stretch or unsteady effects without invalidating the flamelet assumption, as long as these effects do not disrupt the flame front, i.e. as long as they do not quench it. Even scales smaller than the flame front thickness might interact with the flame if their only effect is to thicken the flame front and increase the transport coefficients inside the flame zone (as postulated by Damköhler 1940, see Beer & Chigier 1983). It turns out, as will be seen later, that interactions at the small scales are dominated by viscous and transient effects and induce modifications of the flame structure which are less important than previously thought. This explains why we will focus on the extended flamelet (EF) assumption although we reckon that other authors might want to use other approaches.

The next step is to recognize that flame quenching controls the validity of the extended flamelet assumption. When no quenching occurs in a premixed turbulent flame, the flame zone is 'active' everywhere and features the typical structure of an interface separating fresh unburnt reactants from hot burnt products. Then, it is convenient for practical purposes to introduce the following definition of an extended flamelet (EF) regime (figure 2):

A premixed turbulent reacting flow is in an extended flamelet regime if any line connecting one point in the fresh gases to another point in the burnt products crosses (at least) one active flame front.

When the flame front is only slightly perturbed by the turbulent eddies, the regime corresponds to 'wrinkled flamelets'. In more intense turbulence, pockets of fresh gases in burnt products may exist in an extended flamelet regime as long as each pocket is surrounded by an active flame front. This mode of combustion is of the 'corrugated flamelet' type (Peters 1986).

If the local stretch induced by the turbulent flow on the flame front is sufficiently large and the flame is quenched at a given location, combustion stops in the vicinity of this point and fresh reactants will diffuse into the products without burning. Combustion ceases to take place in thin sheets and the flamelet concepts (laminar or extended) become less adequate. Therefore, quenching in a turbulent premixed flame determines the limit between two essentially different behaviours (i.e. flamelets or no flamelets) and is an important mechanism in the description and modelling of turbulent combustion.

The conditions leading to quenching are usually studied by assuming that reactive elements in the turbulent flame (figure 2) behave like a laminar stagnation-point flame (Bray 1980, 1987). There are, however, many differences between the real flow and this model. First, it is unclear whether the effects of multiple scales acting on a

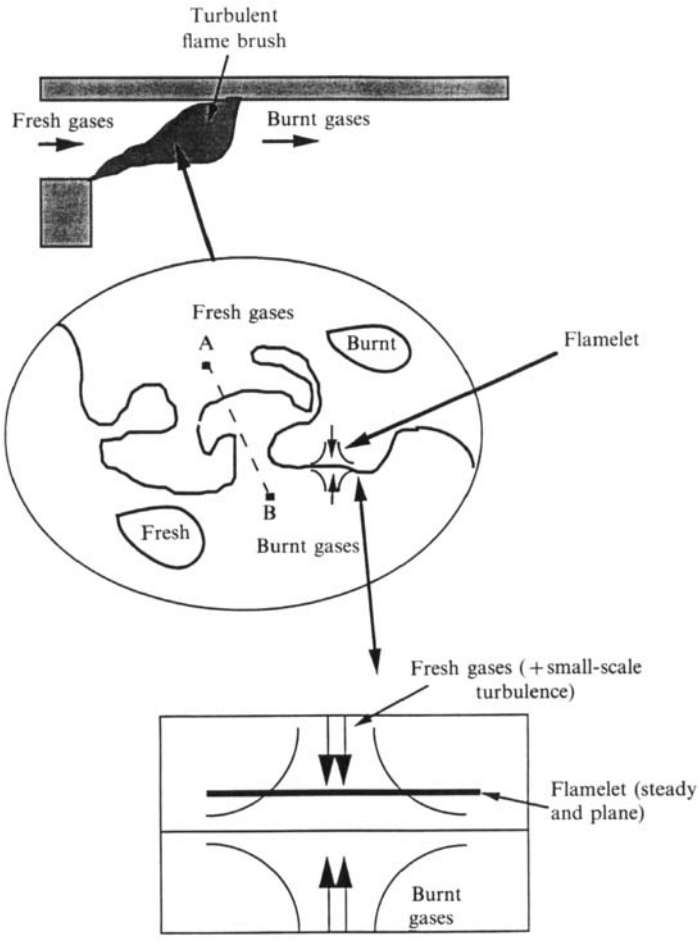

FIGURE 2. The flamelet regime.

flame may be described by an equivalent stretch. Geometrical considerations suggest that, in order to stretch a flame, vortices should be larger than the scales associated with the flame front (typically the thermal thickness of the unstretched flame l_F^u). In this respect, small scales cannot be included in a description which only considers stretch. Furthermore, in a laminar stagnation-point flame, the flame front is planar and submitted to a constant stretch. In a real turbulent flame, the flame front is stretched by turbulent eddies. Because eddies move with respect to the flame, the reaction front is submitted to a variable stretch and it is curved at the same time. As shown by Mikolaitis (1984*a*, *b*), Haworth & Poinsot (1990) and Rutland & Trouvé (1990), the effects of curvature may be quite significant and should be included in the description. Finally, viscous effects may modify the vortex structure and decrease the stretch imposed on the flame front before any quenching takes place. As a result, the interactions between the flame and vortices in the turbulent flow are intrinsically time-dependent. While information obtained from laminar stagnation-point flames submitted to steady stretch with no curvature is certainly of value, it does not completely portray the real flamelets which evolve in a turbulent flame.

The goal of this study is to examine the conditions leading to quenching of a laminar flame front by vortices and thereby deduce new criteria describing the behaviour of premixed flame fronts in a turbulent flow and indicating the limits of

the extended flamelet mode of combustion. This is achieved by performing a detailed analysis of the physical mechanisms controlling turbulent premixed combustion combined with direct numerical simulations of typical aerodynamic interactions. An important feature of this approach is that, using assumptions on flame/turbulence interactions, the problem of quenching in a turbulent reacting stream is reduced to the prediction of quenching of a laminar flame front by a vortex pair. A second feature of this work is the choice of a complete model (including variable density, compressibility, variable diffusion and heat losses) to describe the flow field, but of a simple one-step reaction with an Arrhenius law to represent combustion. This choice is justified by its low computational cost but also by the large amount of theoretical results available on stagnation-point flames (Williams 1985; Bush & Fendell 1970; Libby *et al.* 1983) and curved flames (Mikolaitis 1984*a*, *b*) using one-step chemical models. It is reasonable to start investigating the effects mentioned above (viscous dissipation, time-dependent processes, curvature) in the same framework.

The dimensional arguments used to distinguish different combustion regimes are reviewed in §2. The various forms of the Klimov–Williams criterion for flame quenching are recalled and the classical diagram for premixed combustion is discussed. This section reviews the usual derivation of the Klimov–Williams quenching criterion. An extended dimensional analysis of parameters controlling turbulent premixed flames is developed in the same section. Curvature and viscous effects are taken into account. This analysis reveals some of the questions raised by the Klimov–Williams criterion. A *spectral diagram* concept is introduced to describe the interaction between an isolated vortex pair and a laminar flame front (and not between a complete turbulent field and a flame front). This interaction may be determined exactly from direct simulations.

The basic equations and the simulation method of calculation used to compute vortex/flame interactions are described in §3. The choice of the vortex pair as the most efficient turbulent structure to quench a flame front is discussed as well as the need to take into account heat losses to represent quenching accurately.

Different examples of flame/vortex calculations are presented in §4. Cases where quenching is produced by vortices are effectively obtained. It is shown, however, that viscous dissipation and flame curvature compete with strain and notably affect the quenching processes. The influence of the Lewis number Le is discussed. It is well known that certain dynamical features of laminar flames are controlled by the sign of $Le-1$. Thermo-diffusive instabilities of laminar flames, for example, occur for $Le < 1$ (Zeldovich *et al.* 1980; Williams 1985; Pelce & Clavin 1982) and some of their effects in a turbulent flame will be deduced from the simulations.

A complete spectral diagram is established in §5 for a Lewis number exceeding one ($Le = 1.2$). The behaviour of a complete turbulent reacting flow is inferred and a new turbulent combustion diagram is defined. Different characteristic scales of turbulent premixed combustion are derived. A cutoff scale is defined as the size of the smallest vortex in a given turbulence spectrum having an effect on the flame front. Quenching criteria are also derived and compared with experimental results. When a turbulent field is sufficiently intense to quench the flame front, it is shown that quenching only occurs in a limited range of turbulent lengthscales and that heat losses have a notable influence on the process.

2. Turbulent combustion diagrams

To start the analysis, it is worth recalling some of the ideas which have led to the current classification of turbulent combustion regimes (§2.1). It will then be possible to introduce a new approach to the topic based on the spectral diagram concept (§2.2).

2.1 *The classical approach for turbulent combustion diagrams*

The qualitative nature of turbulent combustion regimes has received considerable attention in the past. An early attempt to distinguish the different flame types is contained in the work of Barrère (1974) who proposed a classification of turbulent flames in terms of two dimensionless groups: the ratio of the turbulence integral scale l to the flame front thickness l_F^u and the ratio of the root-mean-square velocity fluctuations u' to the laminar flame speed s_L^u. (Both l_F^u and s_L^u refer to an unstretched planar laminar flame). Barrère recognized four different regimes: pseudo laminar flames for $l/l_F^u < 1$ and $u'/s_L^u < 1$; wrinkled flames for $l/l_F^u > 1$ and $u'/s_L^u < 1$; volumetric combustion for $l/l_F^u < 1$ and $u'/s_L^u > 1$; pocket flames for $l/l_F^u > 1$ and $u'/s_L^u > 1$.

This view on the qualitative nature of turbulent combustion is shared and discussed in depth by Borghi (1985, 1988) and Peters (1986). A different presentation is put forward by Bray (1980) and Williams (1985). These authors use the turbulence Reynolds number $Re_l = u'l/\nu$ and the Damköhler number $Da = (l/u')/(l_F^u/s_L^u)$ to plot a diagram of combustion regimes. The two representations are in fact equivalent and we here adopt the notations and assumptions of Peters (1986).

In the current form of the combustion diagram different regime transitions may be associated with specific lines (figure 3*a*). (i) The line $u'/s_L^u = 1$ separates the wrinkled and corrugated flame regimes. The latter designates a combination of flame sheets and pockets formed by turbulent fluctuations. (ii) The upper limit of the extended flamelet domain is the limit of interest for the present study. It indicates the appearance of quenching and the validity limits of the flamelet assumption. It is generally believed that a regime of distributed reaction prevails beyond this limit. Quenching is reached when the stretch $(1/A)\,(\mathrm{d}A/\mathrm{d}t)$ (where A is the flame surface) imposed to the flame equals the critical extinction stretch and induces local quenching. The critical stretch depends on the flame characteristics but may be estimated for a planar stagnation point flame by s_L^u/l_F^u (Peters 1986; Bray 1980). Defining the Karlovitz number by

$$Ka = \frac{(1/A)\,(\mathrm{d}A/\mathrm{d}t)}{s_L^u/l_F^u}, \tag{1}$$

and assuming that the turbulent flame front will be quenched for the stretch value that extinguishes a stagnation-point flame, one expects local quenching and distributed reaction zones for $Ka > 1$.

A standard estimate of the typical stretch $(1/A)\,(\mathrm{d}A/\mathrm{d}t)$ may be deduced from the Taylor microscale Λ and from the macroscale velocity fluctuations u' as

$$\frac{1}{A}\frac{\mathrm{d}A}{\mathrm{d}t} \approx \frac{u'}{\Lambda}. \tag{2}$$

It is convenient (but not always appropriate) to describe the turbulent flow field in terms of the Kolmogorov cascade. The dissipation rate ϵ, the Taylor microscale Λ and the Kolmogorov scale η are then given by the following relations:

$$\epsilon = u'^3/l, \quad \Lambda/l = Re_l^{-\frac{1}{2}}, \quad \eta/l = Re_l^{-\frac{3}{4}},$$

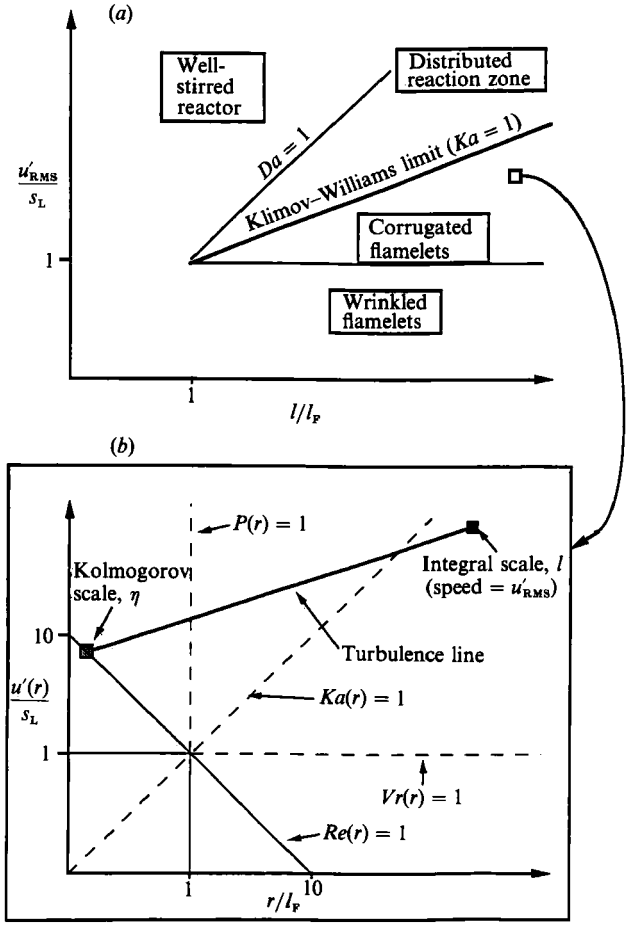

FIGURE 3. (*a*) Standard diagram for turbulent premixed combustion (the diagram is plotted in the form proposed by Peters). (*b*) Spectral diagram principle.

where $Re_l = u'l/\nu$, and ν is the kinematic viscosity. The Kolmogorov characteristic velocity is then related to the macroscale velocity u' by $u_K/u' = Re_l^{-\frac{1}{4}}$. The flame front thickness l_F^u and the flame speed s_L^u are also related by the approximate relation $s_L^u l_F^u/\nu = 1$. Many equivalent forms of the Karlovitz number may be derived from these expressions:

$$Ka = \left(\frac{(u'/s_L^u)^3}{l/l_F^u}\right)^{\frac{1}{2}}, \tag{3}$$

or

$$Ka = \frac{(\epsilon/\nu)^{\frac{1}{2}}}{s_L^u/l_F^u}, \tag{4}$$

or

$$Ka = (l_F^u/\eta)^2, \tag{5}$$

or

$$Ka = \frac{u_K/\eta}{s_L^u/l_F^u}. \tag{6}$$

The Klimov–Williams (KW) criterion is then derived from (5) by stating that flamelets cannot be observed in a reacting flow if the Kolmogorov scale η is smaller than the flame thickness l_F^u. According to this criterion, flamelets cannot exist beyond

$Ka = 1$ because their internal structure is altered by stretching and quenching. It is interesting to note that the derivation starts from a criterion based on an examination of stretch effects ($Ka < 1$) and leads to a criterion based on scales ($\eta > l_F^u$).†

The $Ka = 1$ limit is a line with a $\frac{1}{3}$ slope in figure 3(*a*) (equation (3)). The region lying below $Ka = 1$ corresponds to extended flamelet regimes. According to (6) the critical stretch $(1/A)(dA/dt)$ is the strain rate at the Kolmogorov scale u_K/η. Therefore, the KW criterion involves a single turbulent scale, namely the Kolmogorov scale.

When the turbulence intensity becomes large and the Damsköhler number Da is less than unity, all turbulence times are smaller than the chemical time. In this situation, designated the well-stirred reactor regime, the character of the turbulent reaction flow is not yet well understood (Williams 1985).

As indicated by one of the reviewers, the previous analysis only identifies the general nature of the various modes of combustion and provides order of magnitude estimates. For example, the distribution of strain rates in a turbulent flow will lead to gradual transitions from one regime to the other and not to abrupt changes as suggested by the lines in figure 3.

2.2. *A new approach based on the spectral diagram concept*

The analysis used in the previous section to define the regimes of premixed turbulent combustion raises many questions, in particular as regards the quenching criterion which defines the boundary of the extended flamelet regime. According to (6), the Kolmogorov fluctuations induce flame quenching (and lead to distributed reaction zones) because they generate the highest strain rates but four important points are obviously ignored:

(i) The Kolmogorov scales may be too small compared with the flame front thickness to stretch it effectively (a point already mentioned by Peters 1986).

(ii) As the Kolmogorov scales (η and u_K) and the flame scales (l_F^u and s_L^u) are linked by the same relations to diffusion coefficients ($\eta u_K/\nu \approx l_F^u s_L^u/\nu \approx 1$, where ν is the kinematic viscosity), viscous dissipation will be important for all structures with a scale close to the flame scale. These structures will be dissipated by viscosity before they quench the flame.

(iii) Scales smaller than the flame front thickness will induce high local curvature and associated thermo-diffusive effects which may counteract the influence of strain.

(iv) The interaction between a turbulent eddy and a flame front will be essentially unsteady. The flame response will depend on the time-evolution of the stretch and on the eddy lifetime.

While some time-dependent effects have been studied for planar stagnation-point flames by Carrier, Fendell & Marble (1975), Rutland (1989) and Haworth *et al.* (1988) and for flame/vortex configurations by Marble (1985), Karagozian & Marble (1986) or Laverdant & Candel (1989), little is known about flame quenching in a transient flow field. Using direct simulation, we will derive extinction criteria including viscous, curvature and time-dependent effects.

† It is also worth adding that the condition $\eta > l_F^u$ is used by some authors as the basic definition of the laminar flamelet regime without any reference to stretch effects. In fact, because of viscous and transient effects, the flamelets might preserve their laminar structure even when $\eta < l_F^u$ Haworth & Poinsot 1990; Rutland & Trouvé 1990) and the condition $\eta > l_F^u$ might not be the right criterion to use even for the laminar flamelet assumption. This point was not investigated here because the extended flamelet assumption is more relevant to most practical models for turbulent combustion.

An additional and perhaps more fundamental problem is that the multiscale nature of the flame interaction with the flow field is not well understood. Indeed, the turbulent flow features a complex combination of vortices with scales ranging from the integral scale l to the Kolmogorov scale η. Each of these scales may be characterized by a lengthscale r and a velocity perturbation $u'(r)$ (figure 3*b*). To describe turbulence/combustion interactions, one has to take into account the existence of these various scales in the flow and, accordingly, build for each point of the combustion diagram, a spectral diagram (figure 3*b*). Each point of the standard combustion diagram corresponds to a turbulent flow containing a spectrum of scales. These scales are represented by a set of points in the spectral diagram.

We will assume that the turbulent reference quantities correspond to the fresh gases and that the turbulent spectrum in this part of the flow may be described by the Kolmogorov relation: $u'(r)^3/r = \epsilon$, where r is a lengthscale varying between the Kolmogorov scale η and the integral scale l, and ϵ is the dissipation rate. It is implicitly assumed throughout this paper that turbulence is generated upstream of the flame front, in the fresh gases. A typical example of such a situation is a turbulent flame propagating in a piston engine. Cases where turbulence is generated in the burnt gases, as for example a premixed flame propagating in a shear flow, would require additional studies.

Under this assumption a turbulent flow field is represented in the spectral diagram by a straight line that may be designated as the 'turbulence line' bounded by the integral and Kolmogorov scales. Each scale of the turbulence line will have a different effect on the flame front. Some vortices may induce quenching, some may form pockets of fresh gases surrounded by an active flame sheet without quenching while others may be dissipated by viscous effects before they interact with the flame.

In the same turbulent reacting flow, all three types of vortices may be found at the same time. The flow structure is a complex superposition of all vortices and a description based on a single scale cannot take all mechanisms into account. The three effects (pocket formation, quenching and vortex decay) may be characterized by three dimensionless groups (figure 3*b*) which depend on the lengthscale r under consideration:

(i) $Vr(r) = u'(r)/s_L^u$ is the ratio of the turbulent velocity fluctuations associated with the lengthscale r to the laminar flame speed. A necessary condition for strong interaction (to form a pocket, for example) is that the speed induced by the vortex be greater than the flame speed, i.e. $Vr(r) > 1$.

(ii) $Ka(r) = (u'(r)/r)/(s_L^u/l_F^u) \approx Re_r^{-\frac{1}{2}}(l_F^u/\eta)^2$ is the Karlovitz number for the scale r (Re_r is the Reynolds number associated to the scale r.) $Ka(r)$ coincides with the Karlovitz number of (3)–(6) if one considers the Kolmogorov scale $r = \eta$. A necessary condition for quenching of the flame front by stretching is $Ka(r) > 1$.

(iii) $P(r) = (r^2 s_L^u)/(\nu l_F^u) \approx (r/l_F^u)^2$ is a measure of the vortex power. It is the ratio of the lifetime of the vortex r^2/ν to the chemical time l_F^u/s_L^u. This number may be interpreted as the ratio of the penetration length of the vortex into the flame front (before it is eventually dissipated by viscous effects) to the flame front thickness. Vortices with a power lower than unity ($P(r) < 1$) will be dissipated by viscous effects before they affect the flame front. $P(r)$ is also a good measure of the curvature effects arising from the interaction of a vortex of size r with a flame front of thickness l_F^u.

It is already possible to reconsider the Klimov–Williams criterion. According to this criterion, the Kolmogorov scales are the scales that may quench the flame front. In the spectral diagram (figure 3*b*), the Kolmogorov scales belong to the line $Re_\eta = u'(\eta)\eta/\nu \approx (u'(\eta)/s_L^u)(\eta/l_F^u) = 1$. If the Kolmogorov lengthscale is larger than the

flame thickness ($\eta > l_F^u$), the corresponding flow conditions fall below the line $Vr(r) = 1$. The vortex speed is lower than the flame speed and the interaction is 'weak'. On the other hand, if $\eta < l_F^u$, the power $P(\eta)$ of the vortex is small (although its velocity may be high) and the fluctuation is dissipated by viscous effects before it can interact with the flame. In both cases, Kolmogorov scales are unable to quench a flame front. Clearly, the interaction between a single vortex and a flame front involves more than a single non-dimensional number (for example, the Karlovitz number) and must be studied in more detail.

Now, this interaction may be precisely characterized using direct simulation and an accurate spectral diagram based on calculations of flame/vortex interactions (and not based only on dimensional analysis) may be constructed as shown in §5.

This article will focus on defining quenching and cutoff limits. the formation of pockets will be left for future studies. The quenching limit is of special interest for modelling since it determines the domain of application of extended flamelet models while the cutoff scale is the smallest scale which can affect the flame front. This scale is somewhat related to the Gibson scale (Peters 1986) and may be used as a cut-off scale in fractal theories of turbulent combustion (Gouldin, Bray & Chen 1989; Mantzaras, Felton & Bracco 1989).

3. Direct simulation of vortex/flame front interactions

Studies of vortex/flame interactions initiated by Marble (1985) have been pursued by many authors (Karagozian & Marble 1986; Ashurst *et al.* 1987; Cetegen & Sirignano 1988; Rutland & Ferziger 1989; Laverdant & Candel 1989; Jou & Riley 1989; Ghoniem & Krishnan 1988). While mechanisms like the mutual annihilation of flame surfaces or the suppression of vortex rollup by thermal dilatation have been well described, other features relevant to turbulent combustion are not considered and in particular little is to be found on flame quenching by a vortex.

3.1. *The basic equations*

Asymptotic studies (Williams 1985) show that non-unity Lewis number and non-zero heat losses should be included in a computation aimed at the understanding of quenching. This is done in the present study by solving the Navier–Stokes equations in a two-dimensional configuration under the following assumptions.

We consider a compressible viscous reacting flow. The chemical reaction is represented by a single-step mechanism

$$R\,(\text{reactants}) \rightarrow P\,(\text{products})$$

and the reaction rate $\dot{w}_R$ is expressed as

$$\dot{w}_R = B\rho\, Y_R \exp\left(-\frac{T_a}{T}\right). \tag{7}$$

It is convenient to follow Williams (1985) and cast this expression in the form

$$\dot{w}_R = \mathscr{B}\rho\, Y_R \exp\left(\frac{-B(1-\Theta)}{1-\alpha(1-\Theta)}\right),$$

where Θ is the reduced temperature $\Theta = (T-T_1)/(T_2-T_1)$. T_1 is the fresh gas temperature and T_2 is the adiabatic flame temperature for unity Lewis number. T_a

is the activation temperature. The coefficients $\mathscr{B}$, α and β are, respectively, the reduced pre-exponential factor, the temperature factor and the reduced activation energy:

$$\mathscr{B} = B\exp(-\beta/\alpha), \quad \alpha = (T_2 - T_1)/T_2, \quad \beta = \alpha T_a/T_2. \tag{8}$$

The mass fraction of the reactants Y_R may be conveniently non-dimensionalized by the initial mass fraction of reactants Y_R^0 in the fresh gases: $\tilde{Y} = Y_R/Y_R^0$. $\tilde{Y}$ varies from 1 in the fresh gases to 0 in the burnt gases.

Using these assumptions and a Cartesian frame of reference, the fluid dynamic equations may be cast in the form

$$\frac{\partial \rho}{\partial t} + \frac{\partial}{\partial x_i}(\rho u_i) = 0, \tag{9}$$

$$\frac{\partial \rho E}{\partial t} + \frac{\partial}{\partial x_i}[(\rho E + p)\, u_i] = \frac{\partial}{\partial x_i}(u_j \tau_{ij}) + \frac{\partial}{\partial x_i}\left(\lambda \frac{\partial T}{\partial x_i}\right) + Q\dot{w} - h(T - T_1), \tag{10}$$

$$\frac{\partial \rho u_i}{\partial t} + \frac{\partial}{\partial x_j}(\rho u_i u_j) + \frac{\partial p}{\partial x_i} = \frac{\partial \tau_{ij}}{\partial x_j}, \tag{11}$$

$$\frac{\partial(\rho \tilde{Y})}{\partial t} + \frac{\partial}{\partial x_i}(\rho \tilde{Y} u_i) = \frac{\partial}{\partial x_i}\left(\rho \mathscr{D} \frac{\partial \tilde{Y}}{\partial x_i}\right) - \dot{w}, \tag{12}$$

where

$$\rho E = \tfrac{1}{2}\rho \sum_{k=1}^{3} u_k^2 + \frac{p}{\gamma - 1}, \tag{13}$$

$$\tau_{ij} = \mu\left(\frac{\partial u_i}{\partial x_j} + \frac{\partial u_j}{\partial x_i} - \tfrac{2}{3}\delta_{ij}\frac{\partial u_k}{\partial x_k}\right), \tag{14}$$

$$\dot{w} = \frac{\dot{w}_R}{Y_R^0} = \mathscr{B}\rho\, \tilde{Y} \exp\left(\frac{-\beta(1-\theta)}{1-\alpha(1-\theta)}\right). \tag{15}$$

In these expressions ρ is the mass density, p is the thermodynamic pressure, ρE is the total energy density, Q designates the heat of reaction per unit mass of fresh mixture ($Q = -\Delta h_f^0\, Y_R^0$ where Δh_f^0 is the heat of reaction per unit mass of reactant).

We assume that the gas mixture is a perfect gas with constant molar mass and a specific heat ratio γ of 1.4. The thermal conductivity λ and the diffusion coefficient $\mathscr{D}$ are obtained from the viscosity coefficient μ according to

$$\lambda = \mu C_p/Pr, \quad \mathscr{D} = \mu/(\rho Sc), \tag{16}$$

where the Prandtl number Pr and the Schmidt number Sc are constant. As a consequence the Lewis number $Le = Sc/Pr$ is also constant. The viscosity μ is a function of temperature: $\mu = \mu_1(T/T_1)^b$.

An important part of the model is the presence of volumetric heat losses. Asymptotic analysis (Libby *et al.* 1983; Williams 1985) shows that the temperature of the burnt gases T_2 is directly controlling quenching. *Perfectly adiabatic* flames with realistic Lewis numbers of order 1 will be partially quenched by intense stretch but not completely extinguished. In principle one may speculate that such flames always form flamelets in a turbulent flow! This is not true in practice, because the

temperature of the burnt gases T_2 downstream of the reaction zone is never equal to the adiabatic flame temperature T_a. This may be due to different effects. For example, hot gases may be cooled down by convection against walls and then transported again into the domain where they meet another flame front. In piston engines, the sudden expansion due to exhaust valves opening leads to a large decrease of the burnt gases temperature. Another possibility is the formation of soot and the existence of large radiative heat losses from the burnt gases to the walls. None of these mechanisms is easy to predict but they certainly take place. As a consequence, the temperature of the burnt gases T_2 is always less than the adiabatic temperature and quenching is controlled by this effect. *Therefore, if one wishes to study flame quenching, it is not appropriate to consider adiabatic flames.* For the present work, we have chosen to use strong heat losses to maximize quenching. In configurations described by a more realistic energy balance, quenching will be less likely to occur than in the present work and the extended flamelet assumption will be satisfied in an even broader domain.

Heat losses are included in the energy balance (10) in the form of a linear term $h(T-T_1)$. The heat-loss coefficient is expressed as a function of the reduced activation energy β (Williams 1985):

$$h = \lambda Sc^2(s_L^u/\nu)^2 c/\beta, \tag{17}$$

where c is a dimensionless heat-loss coefficient.

3.2 *The numerical method*

The system (9)–(12) is solved using a high-order finite-difference explicit scheme. The numerical accuracy is sixth order in space and third order in time (Lele 1989, 1990). The spatial derivatives are computed using a compact scheme and the time advancement is produced by a minimal-storage third-order Runge–Kutta scheme (Wray 1990). Boundary conditions are specified using the NSCBC method (Poinsot & Lele 1990). This method uses the right number of boundary conditions required for the reacting Navier–Stokes equations and allows an efficient treatment of non-reflecting boundary conditions so that acoustic waves generated by the vortex/flame interaction do not reflect on boundaries and cannot influence the calculation inside the computational domain. The numerical method has been validated in many different situations such as non-reacting compressible shear layers (Lele 1989), reacting shear layers (Poinsot & Lele 1991) or homogeneous turbulence. Only two-dimensional cases will be used in this study. Typical grids contain 25000 points.

3.3. *The configuration*

The choice of the configuration is an important part of the simulation. Previous studies of vortex/flame interactions have been mainly performed for a single vortex interacting with a flame front while a pair of vortices is considered in the present study (figure 4*a*). The reasons for this choice are as follows:

(i) Vortex pairs (also designated as 'modons') have been observed in many turbulent flows and appear to be a generic structure of turbulent flows (Farge & Sadourny 1989). Two-dimensional simulations of non-reacting turbulent flows show that the interaction of two structures with the same sign leads to fast pairing and alteration of the initial vorticity field (Babiano *et al.* 1987). On the other hand, structures with opposite signs of vorticity may form vortex pairs which travel long distances (because of their self-induced velocity) with little modification of their vorticity field. As far as flame/vortex interactions are concerned, these structures

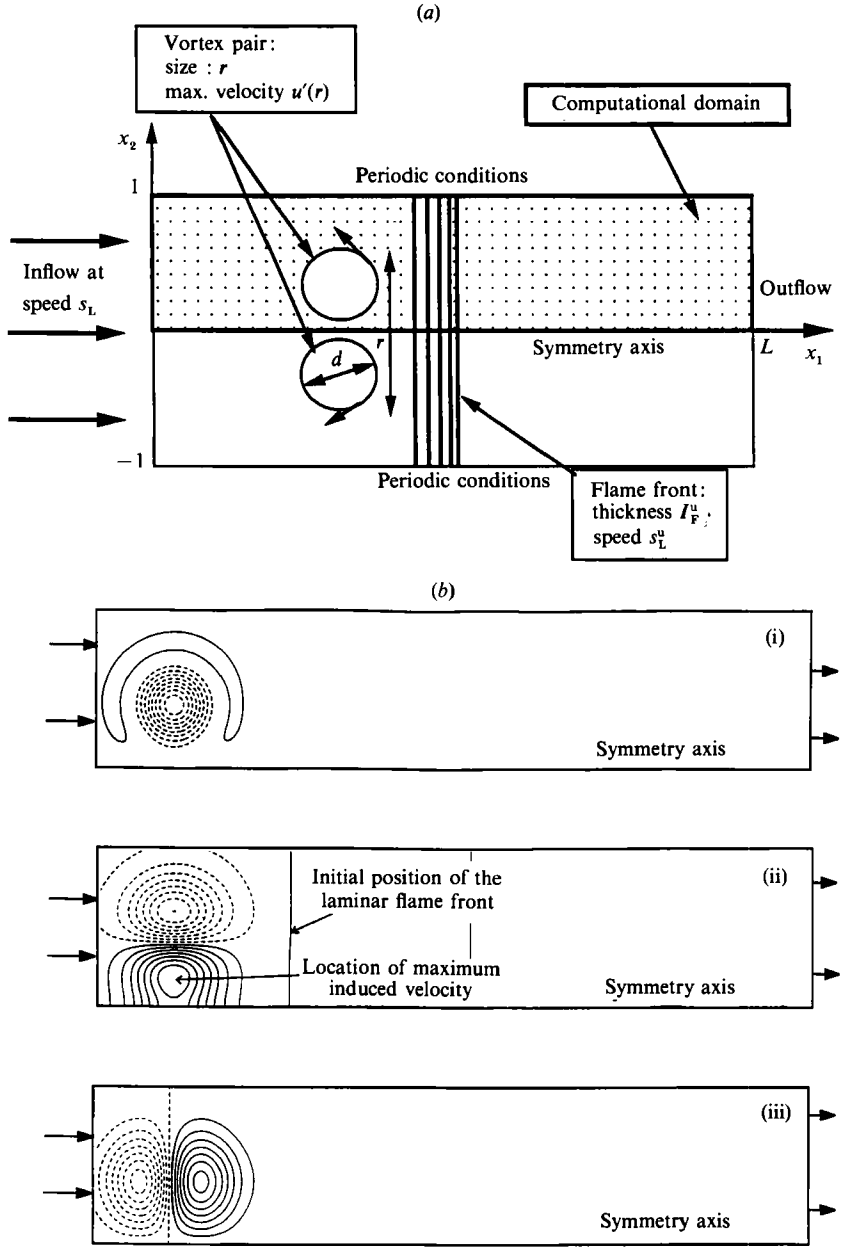

FIGURE 4. (a) Configuration for flame/vortex interactions. (b) (i) Vorticity field ω, $\max|\omega l_F s_L| = 56$; (ii) longitudinal velocity u_1, $\max|u_1/s_L| = 28$; (iii) transverse velocity u_2, $\max|u_2/s_L| = 26$.

have a long lifetime and a high power $P(r)$ (as defined in §2.2) allowing them to interact strongly with the flame front.

(ii) The vortex pair generates a high level of stretch on its axis. Thus, in a given turbulent flow, vortex pairs are among the most efficient structures in terms of flame quenching. In addition, the self-induced velocity field created by the vortex pair entrains the flame towards cooler gases flowing behind the flame front, thereby increasing the effects of stretch and promoting extinction.

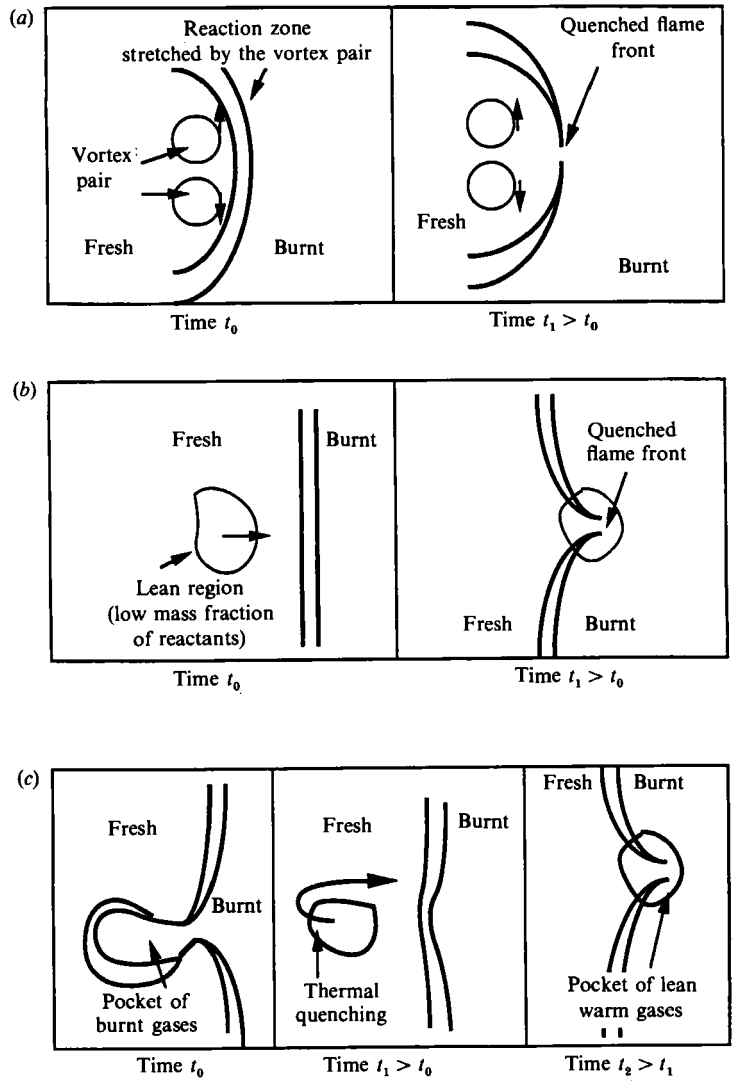

FIGURE 5. Direct and indirect quenching mechanisms in premixed turbulent flames. (*a*) Direct quenching by stretch, (*b*) indirect quenching in non-homogeneous mixtures, (*c*) indirect quenching in homogeneous mixtures.

(iii) Vortex pairs (or vortex rings in three-dimensional geometries) may be easily generated in experiments (Cattolica & Vosen 1987; Jarosinski, Lee & Knystautas 1988).

The basic idea is therefore to assume that among all vortices which may be found in a turbulent field, only vortex pairs need to be considered if one wishes to study quenching. There are probably many possible mechanisms leading to flame quenching in a turbulent flow. In this paper, we will deal only with direct quenching (figure 5*a*) which is obtained by submitting a flame front to an intense stretch, for example to the hydrodynamic field generated by a vortex pair. However, it is also possible to imagine indirect quenching mechanisms where stretch would not play any role. Consider, for example, a non-homogeneous mixture of fresh gases (figure 5*b*). Regions that are depleted of reactants may decrease the reaction rate locally and

quench the flame front (F. E. Marble 1989 private communication). Even for a perfectly homogeneous mixture, a pocket of burnt gases may be separated from the products and isolated in the cold fresh gases (figure 5c). If it is small enough, this pocket may be quenched by thermal effects and mix with surrounding fresh gases, thereby locally lowering the mass fraction of reactant. Later, when this part of the flow enters the flame front, the reactant mass fraction ceases to be homogeneous and a second quenching may happen. Although indirect quenching processes are not unlikely, we consider direct mechanisms to be more important and we will limit this study to them.

This choice is also consistent with the two-dimensional geometry which is used here. It has been shown that flame stretch is essentially characterized by the flow characteristics along the normal to the flame front and that the flow along the two other axis plays little role (Libby & Williams 1987; Rutland 1989). As we are interested in the effects of stretch, using a two-dimensional geometry is a relevant first step. Finally, it is worth noting that the typical lifetime r^2/ν of an isolated vortex in the present two-dimensional computation is longer than the lifetime $u'(r)^2/\epsilon \approx r/u'(r)$ of a vortex of the same size in a real three-dimensional turbulent flow. In general, the present results represent the maximum possible effect of a vortex on a flame front. However, there is one case which could prove this conclusion wrong: a small vortex tube being stretched while it interacts with the flame front would have a lifetime and a vorticity which might be larger than in our two-dimensional case. In the absence of a precise knowledge of vortex tubes in terms of lifetimes and distribution in three-dimensional turbulence, this question remains open and we reckon that it might modify the conclusions of the present work.

The initial configuration is sketched in figure 4(a). Two counter-rotating vortices are created at $t = 0$ on the upstream side of a laminar flame front. As the flow is symmetrical with respect to the x-axis, only the upper part is calculated and displayed. The inlet flow speed u_0 is equal to the laminar flame speed so that the flame does not move when it is not perturbed. The velocity field corresponding to each vortex is initialized at $t = 0$ using the stream function ψ for an incompressible non-viscous vortex (the coordinate origin is located on the vortex centre):

$$\begin{pmatrix} u_1 \\ u_2 \end{pmatrix} = \begin{pmatrix} u_0 \\ 0 \end{pmatrix} + \frac{1}{\rho} \begin{pmatrix} \dfrac{\partial \psi}{\partial x_2} \\ -\dfrac{\partial \psi}{\partial x_1} \end{pmatrix}, \quad \psi = C \exp\left(-\frac{x_1^2 + x_2^2}{2R_c^2} \right). \tag{18}$$

C determines the vortex strength. R_c is the vortex radius (Rutland & Ferziger 1989). Figure 4(b) presents the fields of vorticity $\omega(x, y, t = 0)$, longitudinal velocity $u_1(x, y, t = 0)$ and transverse velocity $u_2(x, y, t = 0)$ for $r/l_F^u = 4.8$ and $u'(r)/s_L^u = 28$. Dashed lines indicate negative values. The maximum velocity $u'(r)$ used to characterize the pair is obtained in this case close to the axis for u_1. The lengthscale r used to characterize the vortex pair is the sum of the vortex diameter d and the distance between vortex centres (figure 4a).

Typical calculations have been performed for $0.8 < r/l_F^u < 12$ and $0. < u'(r)/s_L^u < 100$. Corresponding Reynolds numbers of the vortex pair ($u'(r)\, r/\nu$) vary between 0 and 3000. Note that since we solve for only one vortical structure, the maximum Reynolds number reached in these computations may take relatively high values.

3.4. *Flame stretch and flame speeds*

Flame front dynamics are often described in terms of flame speed. For a premixed flame, two flame speeds may be defined (i) The displacement speed S_d is the speed at which the flame is moving along its normal with respect to the flow of fresh gases. (ii) The consumption speed S_c is the speed corresponding to the mass flow rate of fresh gases consumed through the flame front and is defined by

$$\rho_u^0 Y_R^0 S_c = \int_{-\infty}^{+\infty} \dot{w}\, dn, \tag{19}$$

where $\dot{w}$ is the mass of reactant consumed per unit volume and unit time and ρ_u^0 is the density of the unburnt gases. The integration in (19) is performed along the normal n to the flame front.

In the case of a planar steady laminar flame, these two quantities are equal to the unstretched planar laminar flame speed s_L^u ($S_d = S_c = s_L^u$). In more general situations (for example, for strongly curved flames) S_d and S_c may be very different. For flame tips of Bunsen burners, values of S_d/s_L^u of the order of ten are easily reached (Lewis & Von Elbe 1987) while S_c/s_L^u remains close to unity (Poinsot, Echekki & Mungal 1991).

A flame front propagating in a non-uniform flow is submitted to strain and curvature effects which lead to changes in the flame area A (Williams 1985; Matalon 1983). These changes are measured by the flame stretch $(1/A)(dA/dt)$. A simple general expression of the flame stretch is (Candel & Poinsot 1990):

$$\frac{1}{A}\frac{dA}{dt} = \nabla_t \cdot \boldsymbol{v} - S_d \nabla \cdot \boldsymbol{n}. \tag{20}$$

where $\boldsymbol{v}$ is the flow velocity and $\nabla_t \cdot \boldsymbol{v}$ is the strain in the plane parallel to the flame front. $\boldsymbol{n}$ is the vector normal to the flame front, directed from the fresh gases towards the burnt products. For two-dimensional configurations and flames which are convex towards the fresh gases, the term $\nabla \cdot \boldsymbol{n}$ is the inverse of the radius of curvature R. Therefore, the flame stretch is the sum of two terms: the first term $\nabla_t \cdot \boldsymbol{v}$ represents the effects of strain and is due to the flow non-uniformities while the second $S_d \nabla \cdot \boldsymbol{n} = S_d/R$ represents the effects of curvature. When $(1/A)(dA/dt) > 0$, the flame front is positively stretched (in most cases, we will call it only 'stretched'). The simplest example of positively stretched flame is the planar stagnation point flame. When $(1/A)(dA/dt) < 0$, the flame front is negatively stretched (we will call is 'compressed'). A typical example of compressed flame is a flame front curved towards the fresh gases.

It is important to remember that stretch includes the effects of strain as well as those of curvature. This point may lead to some confusion regarding the effects of these parameters. Two different questions must be answered:

(i) Is stretch the only parameter needed to characterize the behaviour of a flamelet? In the case of small stretch values, asymptotic studies show that stretch is, indeed, the only scalar controlling the displacement flame speed (Clavin & Williams 1982; Clavin & Joulin 1983) but the extension of this result to high stretch values has no rigorous basis. Furthermore, this relation has been derived for the displacement speed but no result is available for the consumption speed, which is the quantity of interest in flamelet models (Candel *et al.* 1990; Cant & Bray 1988).

(ii) If the answer to question (i) is positive, what is the most important parameter in stretch: strain or curvature?

Most flamelet models for premixed turbulent combustion (Williams 1985; Candel *et al.* 1990; Cant & Bray 1988) consider that (i) stretch is the only parameter controlling flame dynamics but also that (ii) curvature has a negligible contribution to stretch in (20). In such models, the flame front is viewed as a collection of strained planar laminar stagnation point flames. The same idea was used in the analysis performed in §2.1 to derive the Klimov–Williams criterion: (i) only stretch was considered and (ii) stretch was assumed to be equal to strain with no correction provided for curvature. To be rigorous, the word stretch used in §2.1 should be replaced by 'strain' because stretch was not estimated in this analysis. One of the goals of the present work will be to investigate questions (i) and (ii) using direct simulations.

From (20), we can rewrite the Karlovitz number given by (1):

$$Ka = \frac{(1/A)\,(\mathrm{d}A/\mathrm{d}t)}{s_{\mathrm{L}}^{\mathrm{u}}/l_{\mathrm{F}}^{\mathrm{u}}} = \frac{l_{\mathrm{F}}^{\mathrm{u}}}{s_{\mathrm{L}}^{\mathrm{u}}}\left(\nabla_t \cdot \boldsymbol{v} - \frac{S_{\mathrm{d}}}{R}\right). \tag{21}$$

We will compute the Karlovitz number Ka and the consumption flame speed S_{c} on the symmetry axis of the computational domain (figure 4*a*) to examine the relationship between flame stretch and the consumption flame speed.

Note that the flame stretch and the Karlovitz numbers ((20) and (21)) are defined for flames which are thin compared to the flow scales, i.e. for an infinitely fast chemistry. With finite-rate chemistry, as will be the case in this work, the evaluation of stretch requires us to define in which plane we estimate the terms of (20). In this paper, the strain term $\nabla_t \cdot \boldsymbol{v}$ is evaluated at the location of maximum reaction rate. The displacement speed is obtained by subtracting the speed of the flame front (measured from the simulation) from the flow speed upstream of the thermal zone. We will use these estimates for our simulations as long as the evaluation of the flame displacement speed S_{d} and the flame curvature R can be done without ambiguity. For flames interacting with small vortices (like in §4.2.2), the Karlovitz number of (21) becomes less significant. This corresponds to the fact that a flame can be 'stretched' only by structures whose characteristic size is greater than the flame thickness.

4. Examples of flame/vortex interactions

This section presents typical aerodynamical interactions between a vortex pair and a laminar flame front. To start the simulation, the structure of the unstretched laminar flame is required. This structure is computed using a one-dimensional version of the code. The initialization of this one-dimensional computation corresponds to an adiabatic flame ($c = 0$) with unity Lewis number ($Le = 1$) and constant viscosity and diffusion coefficients ($b = 0$). The values of Le, b and c are then assigned and a new steady state is reached, providing the unperturbed one-dimensional flame structure. Table 1 gives the values of the laminar flame speed $s_{\mathrm{L}}^{\mathrm{u}}$, of the maximum reaction rate $\dot{w}_{\max}^{\mathrm{u}}$ and of the maximum temperature T_2^{u} corresponding to a plane flame for different values of Le, b and c. The other coefficients are fixed: $Pr = 0.75$, $\alpha = 0.75$ and $\beta = 8$. The parameters $s_{\mathrm{L}}^{\mathrm{u}}$, $\dot{w}_{\max}^{\mathrm{u}}$ and T_2^{u} are normalized by their values s_{L}^{0}, $\dot{w}_{\max}^{0}$ and T_2 for the adiabatic flame with constant diffusion coefficient and unity Lewis number. Two Lewis numbers, 1.2 (§4,1) and 0.8 (§4.2), are considered in this study. For both cases, the heat-loss coefficient is $c = 10^{-4}$ and the temperature exponent of the viscosity is $b = 0.76$.

Adiabatic flame + constant diffusion coefficients ($c = 0$, $b = 0$)			
Lewis number	0.8	1.0	1.2
s_L^u/s_L^0	0.935	1.0	1.069
T_2^u/T_2	1.0	1.0	1.0
$\dot{w}_{max}^u/\dot{w}_{max}^0$	0.89	1.0	1.08
Adiabatic flame + variable diffusion coefficients ($c = 0$, $b = 0.76$)			
Lewis number	0.8	1.0	1.2
s_L^u/s_L^0	1.52	1.59	1.69
T_2^u/T_2	1.0	1.0	1.0
$\dot{w}_{max}^u/\dot{w}_{max}^0$	0.90	1.0	1.18
Non adiabatic flame + variable diffusion coefficients ($c = 0.0001$, $b = 0.76$)			
Lewis number	0.8	1.0	1.2
s_L^u/s_L^0	0.99	1.21	1.36
T_2^u/T_2	0.923	0.941	0.95
$\dot{w}_{max}^u/\dot{w}_{max}^0$	0.43	0.61	0.78

TABLE 1. Laminar flame computations for $\alpha = 0.75$, $\beta = 8.0$ and $Pr = 0.75$

4.1. *Flame/vortex interactions for Le = 1.2*

First consider the case of a Lewis number larger than unity ($Le = 1.2$). In this case, a positive flame stretch induces a decrease of the flame speed (figure 1). The flame speed s_L^u is given by $s_L^u/a = 0.0136$, where a is the sound speed. The speed of the corresponding adiabatic flame with constant diffusion coefficient is $s_L^0/a = 0.01$ (table 1) and the pre-exponential constant $\mathscr{B}$ is 130.

The unperturbed laminar flame structure is displayed in figure 6. The flame front thickness l_F^u is $3.7\nu/s_L^u$ (l_F^u is defined by $l_F^u = (T_2^u - T_1)/\mathrm{Max}\,(\mathrm{d}T/\mathrm{d}x)$. The 3.7 factor appears because the viscosity is not constant and because the Lewis number differs from unity). The temperature variation of the diffusion coefficient increases the flame speed while heat losses decrease it. Heat losses are quite high, as shown in figure 6(*a*). The reduced temperature $\Theta = (T - T_1)/(T_2 - T_1)$ reaches a maximum of $(T_2^u - T_1)/(T_2 - T_1) = 0.95$ in the reaction zone (instead of 1 for an adiabatic flame) and decreases rapidly downstream to reach 0.6 at the downstream boundary. The maximum reaction rate $\dot{w}_{max}^u$ is $0.78\dot{w}_{max}^0$.

From the large set of simulations, three examples of interactions have been selected. In the first case (§4.1.1) the characteristics of the vortex pair are such that quenching of the flame front is obtained. This example shows that stretch induced by vortices may effectively quench a flame front and thereby supports the analogy between laminar stagnation-point flames and turbulent flames. Another outcome of the interaction is described in §4.1.2 where a pocket is formed without quenching the flame front. This case reveals that the quenching process is, indeed, controlled by the value of the Karlovitz number, at least for large vortices. However, the simulation shows that the interaction may involve more than strain effects. It is then shown in §4.1.3 that curvature and viscous dissipation also play important roles when the vortex size diminishes.

4.1.1. *Flame quenching by a vortex pair for Le = 1.2.*

We consider first a case where the vortex pair size and speed are sufficiently large to induce quenching of the flame front ($r/l_F^u = 4.8$ and $u'(r)/s_L^u = 28$). Figures 7 and 8 display the reaction rate ($\dot{w}$) and the temperature fields at four instants. The temperature is non-dimensionalized using the fresh mixture temperature T_1 and the

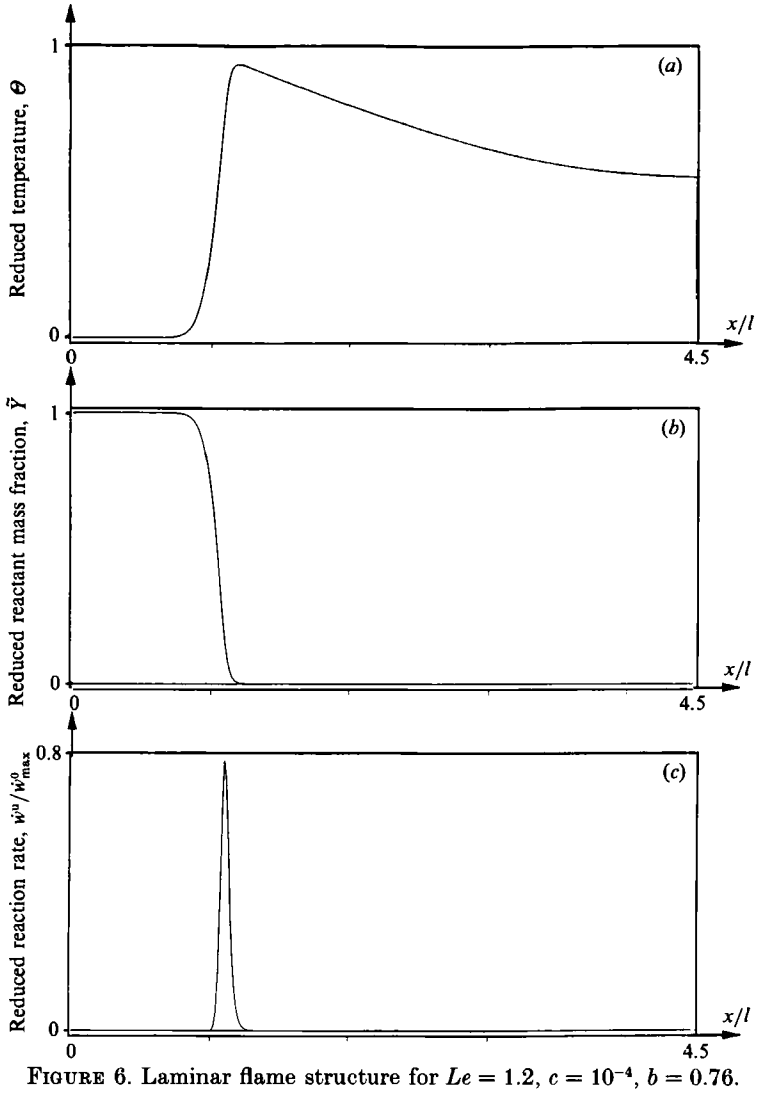

FIGURE 6. Laminar flame structure for $Le = 1.2$, $c = 10^{-4}$, $b = 0.76$.

maximum temperature T_2^u for the laminar unstretched flame given in table 1. Time is normalized by the characteristic time of the flame $\tau_F^u = l_L^u/s_L^u$: $t^+ = ts_L^u/l_F^u$. τ_F^u will be designated as the 'flame time' throughout this paper. At each instant, the maximum values of $\dot{w}/\dot{w}_{max}^u$ (figure 7) and of T/T_2^u (figure 8) are given next to the corresponding graphs.

The interaction is fast and ends after about two flame times. At $t^+ = 0.8$, the vortex pair has stretched and curved the flame but its inner structure is preserved. No quenching is observed (figure 7*a*). At $t^+ = 1.6$, quenching appears on the downstream side of the pocket of fresh gases formed by the vortex pair. These gases are pushed rapidly into regions where the burnt gases have been cooled because of heat losses (figure 8*b*). This effect, combined with the high positive stretch generated by the vortices, causes a nearly complete extinction of the pocket after it has been separated from the bulk of the fresh gases (figure 7*c*). At times $t^+ = 2.0$ and 2.4, the pocket of fresh gases is convected through the burnt gases without burning except near its tail (figures 7*d* and 8*d*).

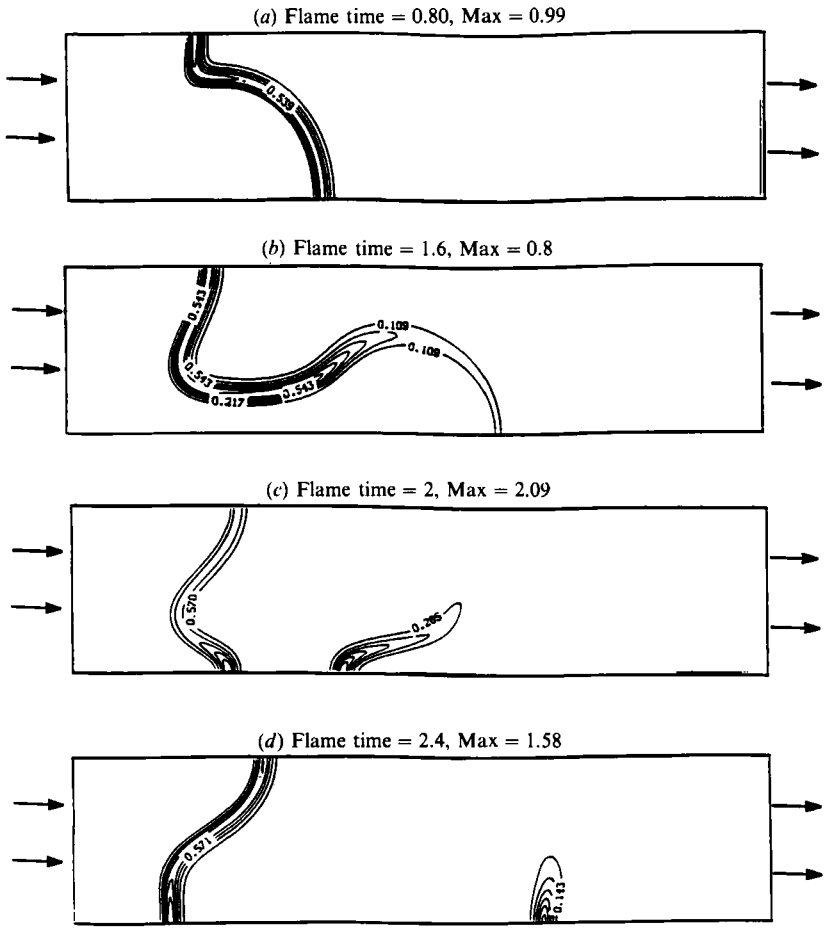

FIGURE 7. Reaction rate fields at four instants for an interaction leading to quenching with $Le = 1.2$ ($r/l_F^u = 4.8$ and $u'(r)/s_L^u = 28$).

Instantaneous characteristic values of combustion may be evaluated on the symmetry axis: the Karlovitz number Ka, the maximum reaction rate and the consumption flame speed S_c are respectively displayed in figures 9(*a*), 9(*b*) and 9(*c*). The Karlovitz number is defined by (21) and its expression requires calculations of the displacement speed and of the radius of curvature of the front. Because of the high computational cost of these estimates, the Karlovitz is computed only at certain instants of the computation. The flame speed S_c is defined by (19) where the integration limits are $x_1 = 0$ and $x_1 = L$. It is meaningful when a single flame front crosses the symmetry axis. After the flame fronts which were wrapped around the vortex merge on the axis (figure 7*c*), this quantity loses its initial meaning.

The absolute maximum reaction rate in the complete flow field is also displayed in figure 9(*b*). The reaction rate and the flame speed in figures 9(*b*) and 9(*c*) are normalized by their unstretched values $\dot{w}_{max}^u$ and s_L^u. After $t^+ = 0.8$, the Karlovitz number evaluated on the symmetry axis is larger than unity (figure 9*a*). However, the flame speed is still 0.6 times its unstretched value (figure 9*c*). For such a Karlovitz number, an analysis based on steady planar stagnation-point flames with heat losses would predict complete extinction (figure 1). The fact that the flame still exists (figure 7*a*) despite such a high Karlovitz number illustrates the importance of

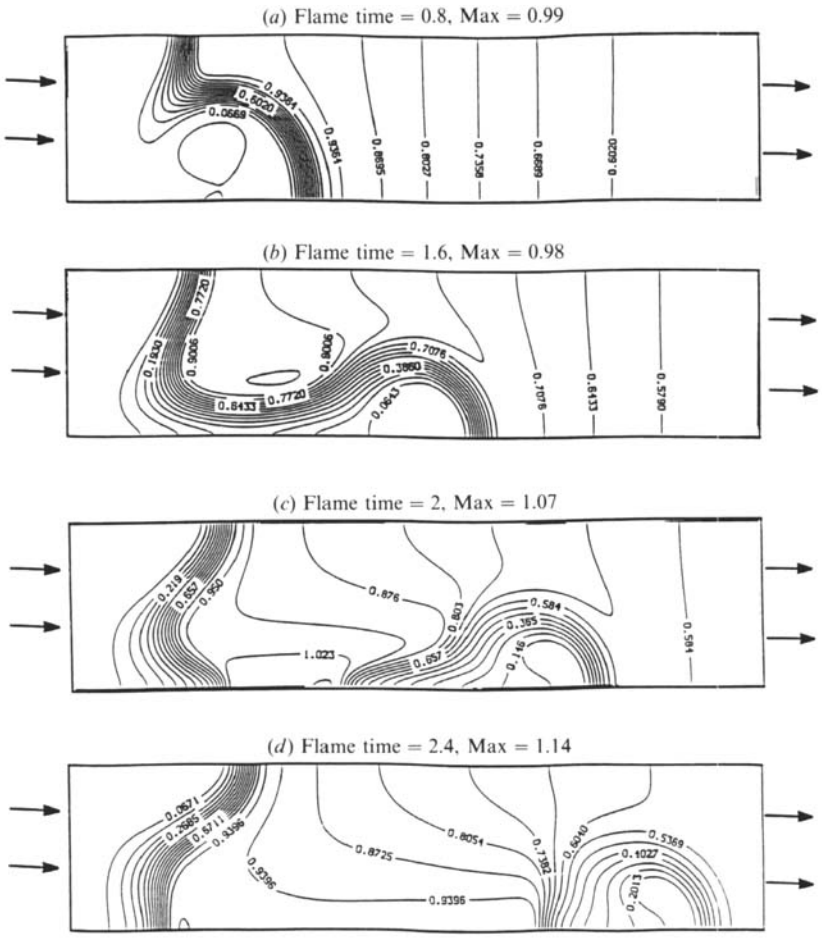

FIGURE 8. Temperature fields at four instants for an interaction leading to quenching with $Le = 1.2$ ($r/l_F^u = 4.8$ and $u'(r)/s_L^u = 28$).

transient dynamics: the flame speed decreases more slowly than the flame stretch increases. Eventually, as the Karlovitz number reaches 3 at $t^+ > 1.5$, the flame is pushed towards cooler gases (figure 8*c*) and complete extinction occurs at $t^+ \approx 1.8$ (figure 9*c*). This interruption of combustion on the symmetry axis is only temporary because the tails of the flame, which have been wrapped around the vortex pair, merge on the axis and allow the flame front to reconnect (figures 7*b* and 7*c*). However, the pocket of fresh gases trapped in the products does not immediately reignite because it is surrounded by gases whose temperature is lower than the adiabatic temperature.

A remarkable feature of this case is that the flame is not only quenched locally by the vortex pair but that some of the unburnt mixture is also able to cross the reactive front. Although the flame front is reconnected at $t^+ = 2$, this configuration is not of any flamelet type as defined in §1. It is possible to go from a point A (in the pocket of fresh gases trapped in the products), to a point B (in the burnt products) without crossing an active flame front (figures 7*d* and 8*d*). This flow does not belong to the flamelet class because the interface between fresh and burnt gases does not coincide with the flame front.

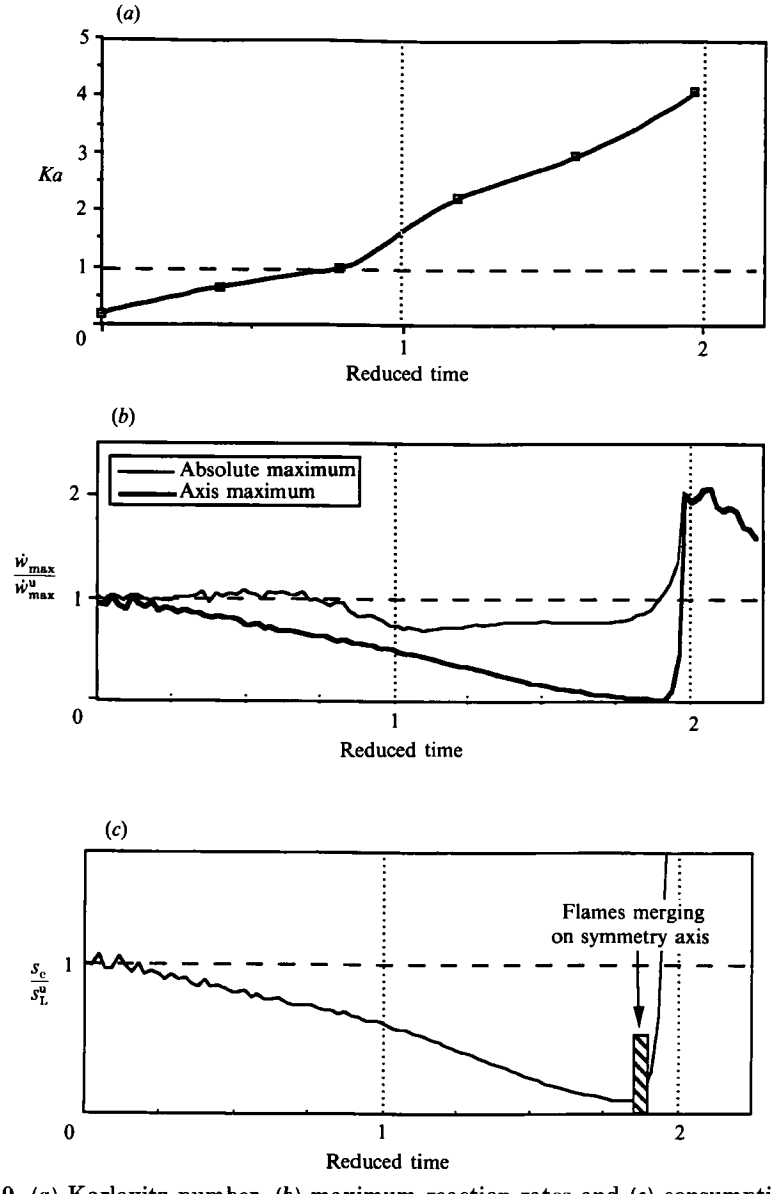

FIGURE 9. (*a*) Karlovitz number, (*b*) maximum reaction rates and (*c*) consumption flame speed on the symmetry axis for an interaction leading to quenching with $Le = 1.2$ ($r/l_F^u = 4.8$ and $(u'(r)/s_L^u = 28)$.

In practice, the mechanism described in this subsection could be responsible for some of the pollutant formation in turbulent flames (i.e. the presence of unburnt hydrocarbons in automobile exhausts). Note also that the unburnt mixture which has crossed the flame front will mix later with the burnt gases behind the front without burning, thereby lowering the product stream temperature even more and promoting faster quenching for other turbulent structures. As a result, the local quenching mechanism described here might eventually lead to a complete quenching of the turbulent flame. The transition from a locally quenched flame front to global extinction depends on the number of vortices interacting with the flame front per

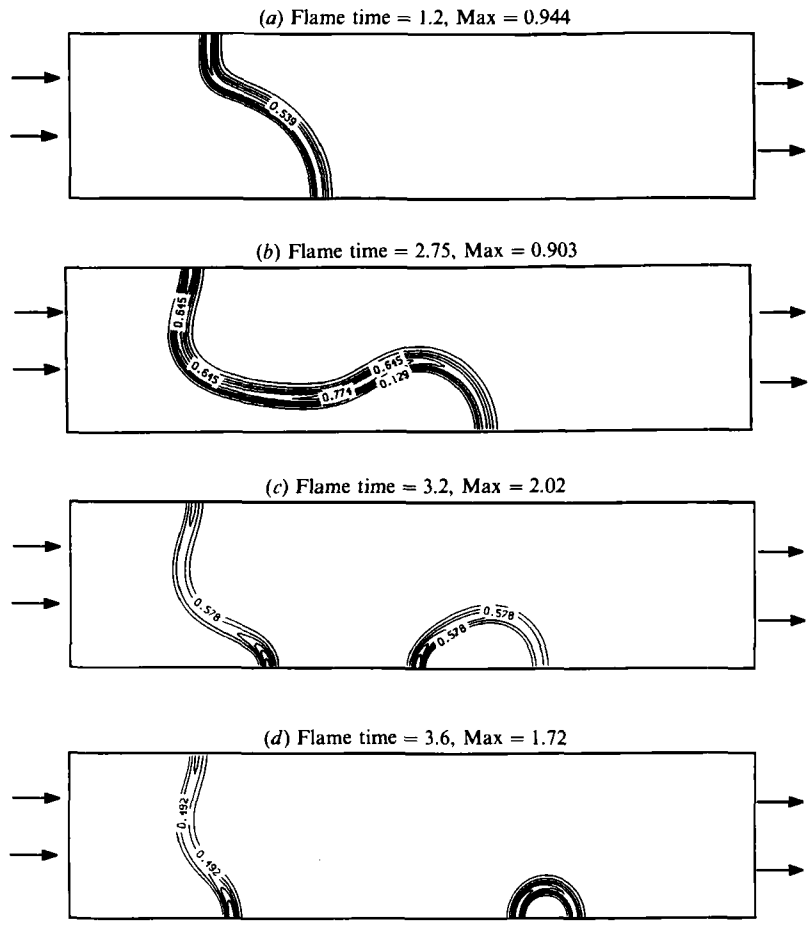

FIGURE 10. Reaction rate fields at four instants for an interaction leading to pocket formation with $Le = 1.2$ ($r/l_F^u = 5$ and $u'(r)/s_L^u = 12$).

unit time (or on the energy spectrum of the turbulent flow). Such statistics may be evaluated using a multi-fractal approach to construct a model for global quenching (Meneveau & Poinsot 1991). However, the precise limit for which local quenching leads to global extinction needs more investigation. For example, direct simulations of fully turbulent reactive flows or experiments with a collection of vortices interacting with a laminar flame front would be of great interest.

While the flame front is stretched on the symmetry axis, it is also compressed at the same time in other regions of the flow (figure 7 and 8). The latter process has small effects in the present case ($Le = 1.2$). The absolute maximum reaction rate (figure 9*b*) only slightly exceeds unity. The vortex pair quenches the flame front on the axis without increasing the reaction rate in other parts of the flow. The total reaction rate in the computation domain increases during the interaction: the flame speed is locally lower on the axis but the available flame surface notably exceeds that corresponding to an unstrained flame. For the present case, the maximum total reaction rate occurs at a flame time $t^+ = 2.5$ and reaches 4 times its unperturbed value.

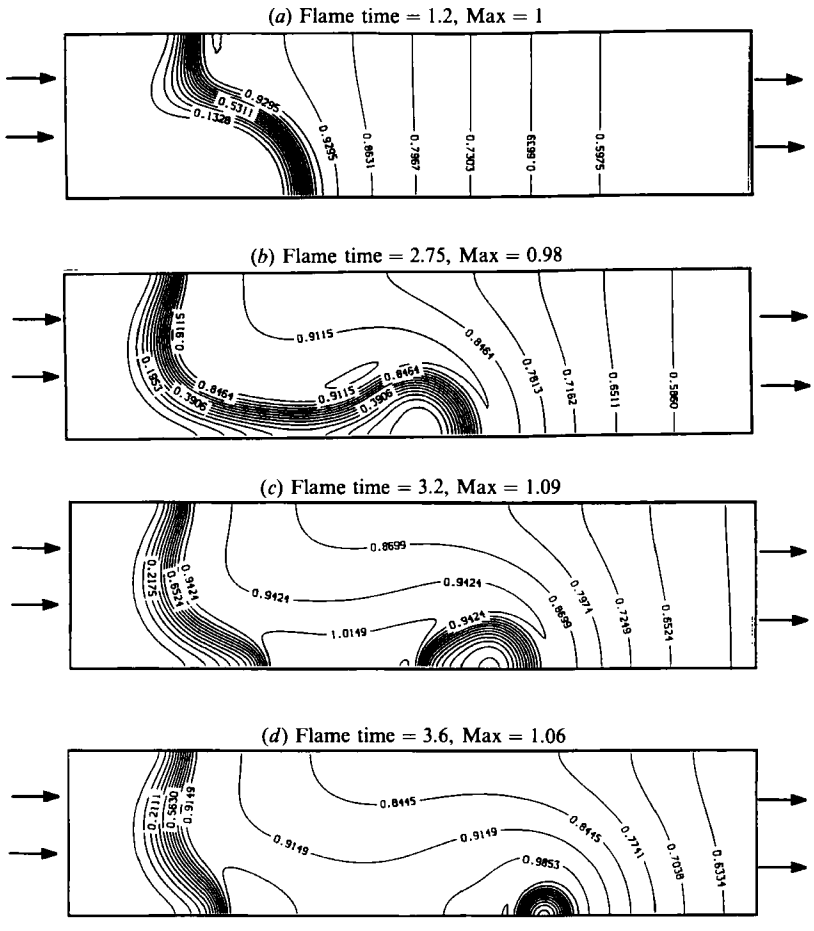

FIGURE 11. Temperature fields at four instants for an interaction leading to pocket formation with $Le = 1.2$ ($r/l_F^u = 5$ and $u'(r)/s_L^u = 12$).

4.1.2. *Pocket formation without quenching for* $Le = 1.2$

In the previous example, a pocket of unburnt gases was created by a local quenching of the flame front. Pocket formation may also occur without quenching. For a vortex pair of the same size as before but with a lower rotation speed ($r/l_F^u = 5$ and $u'(r)/s_L^u = 12$), a pocket of fresh fluid is created in the burnt stream (figure 11) but this pocket is surrounded by an active flame front which is never quenched (figure 10). The pocket created at $t^+ \approx 2.3$ is pushed into the burnt gases but its border is not stretched enough to be quenched (figure 10*c*). The fresh gases contained in the pocket in figures 11(*c*) and 11(*d*) are rapidly consumed as they are convected downstream. This configuration belongs to the regime of corrugated flame sheets.

Time variations of the Karlovitz number on the axis (figure 12) show a maximum value around 1. After $t^+ = 1.2$, the Karlovitz number decreases and reaches negative values, indicating that the flame is slightly compressed. This is due to the fast decay of the strain term and to the increase of the curvature term in (21). This behaviour differs from that presented in the previous section. Here, the initial straining field is too weak to quench the flame front before it becomes strongly curved. After $t^+ = 1.2$, the radius of curvature is small enough to prevent quenching. The minimum flame speed on the axis is 0.7 times the unperturbed flame speed (figure 12*c*) and the

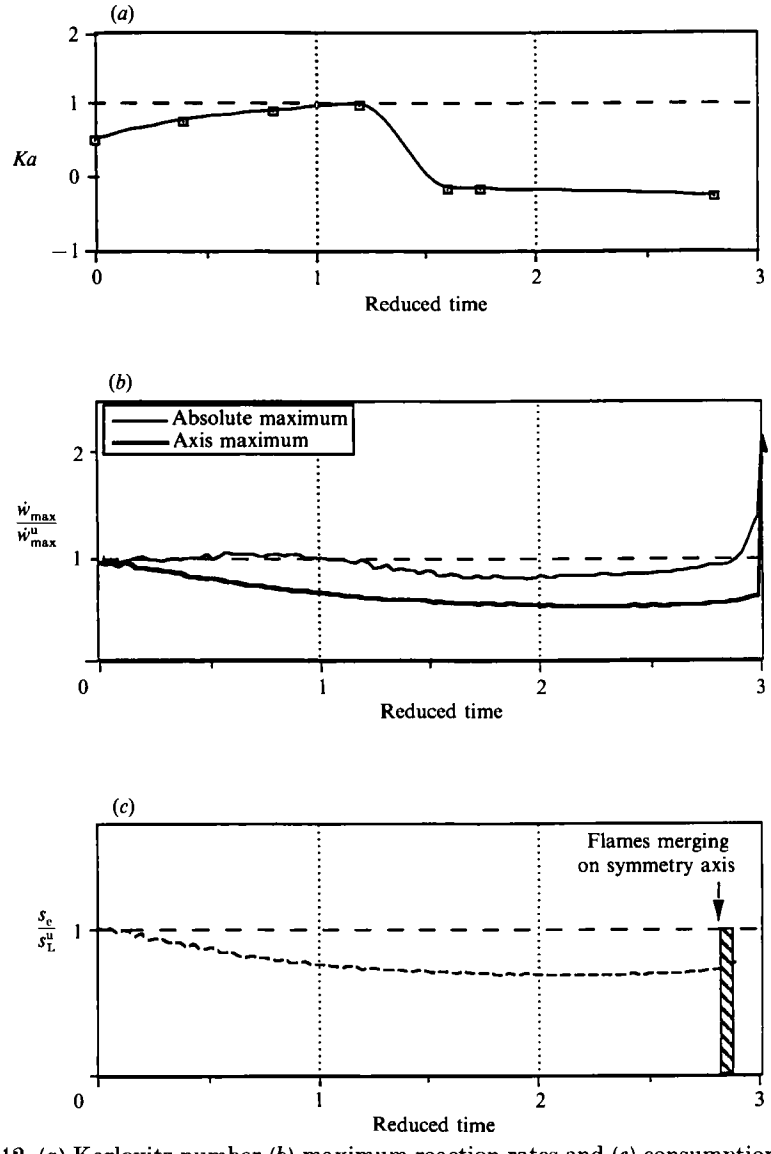

FIGURE 12. (*a*) Karlovitz number (*b*) maximum reaction rates and (*c*) consumption flame speed on the symmetry axis for an interaction leading to pocket formation with $Le = 1.2$ ($r/l_F^u = 5$ and $u'(r)/s_L^u = 12$).

maximum reaction rate on the axis is reduced by only 50% (figure 12*b*). A comparison between this case and the previous one shows that $Ka(r) = 1$ seems to indicate the quenching limit. In §4.1.1, the Karlovitz number reaches 1 rapidly and continues to grow until quenching is obtained while the present case gives a maximum Karlovitz number of 1 and no quenching is observed. However, time-dependent effects delay the response of the flame, and curvature clearly plays an important role. Therefore, the quenching limit $Ka(r) = 1$ is valid only for large vortices, which have a long lifetime and induce little flame curvature, as will be shown in the next section.

The present case also shows that the pocket of fresh gases in the burnt stream is

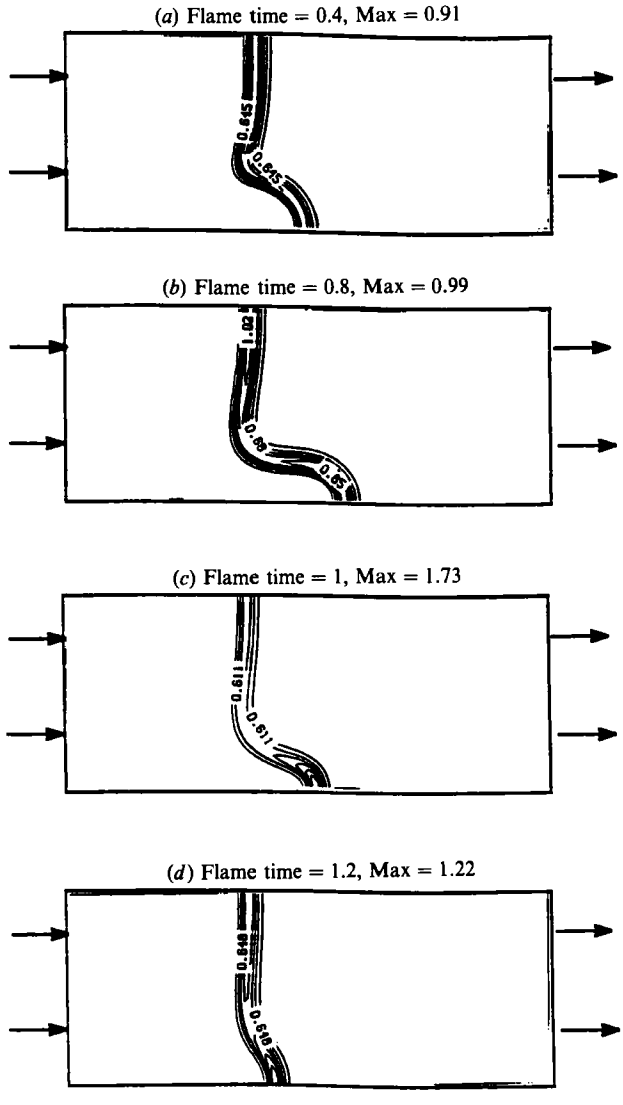

FIGURE 13. Reaction rate fields at four instants for an interaction where curvature prevents quenching with $Le = 1.2$ ($r/l_F^u = 1.6$ and $u'(r)/s_L^u = 28$).

not submitted to quenching because it is strongly curved. This suggests that only small pockets of fresh gases can be formed without quenching the flame front (at least locally).

4.1.3. *The effect of curvature and viscosity for Le = 1.2*

The occurrence of quenching is a strong function of the turbulent eddy size. Large vortices always lead to quenching if their characteristic stretch is higher than the extinction stretch ($Ka(r) > 1$). However, when the vortex-pair size diminishes, thermo-diffusive processes and viscosity effects become significant.

For a Lewis number of 1.2, thermo-diffusion effects are stabilizing. They inhibit the formation of pockets of fresh gases inside the burnt gases by increasing the flame speed at the time of flame fronts which are convex with respect to the fresh gases.

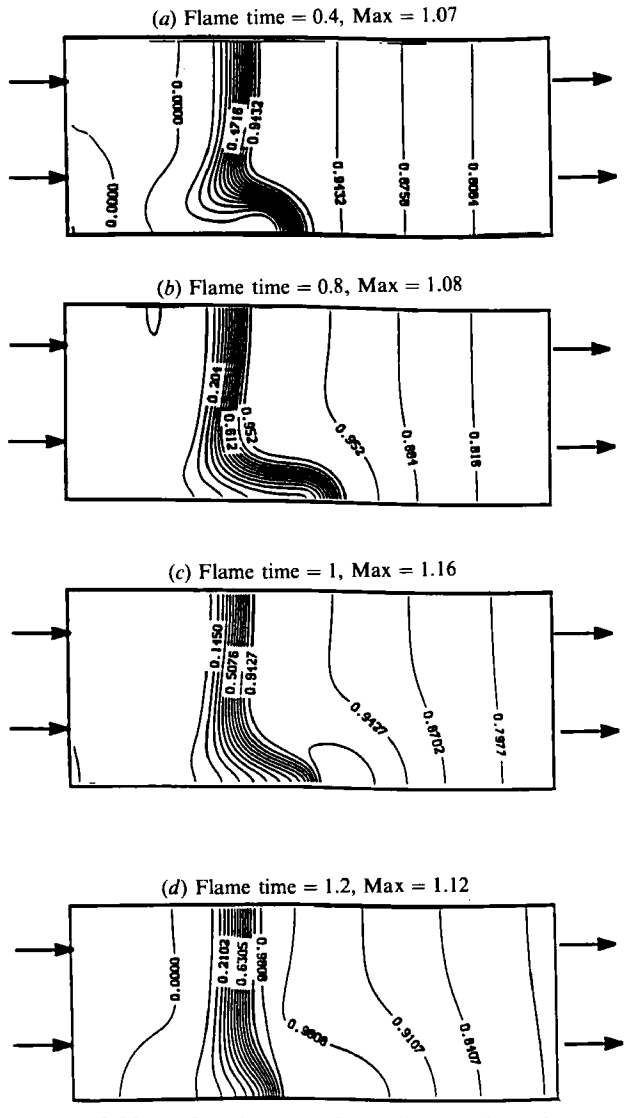

FIGURE 14. Temperature fields at four instants for an interaction where curvature prevents quenching with $Le = 1.2$ ($r/l_F^u = 1.6$ and $u'(r)/s_L^u = 28$).

Simulations show that, when r/l_F^u decreases, local quenching of the flame front becomes more difficult because the flame speed is increased by curvature but also because vortices are rapidly dissipated by viscosity. The flame speed decrease related to strain is compensated by the flame speed increase due to the stabilizing effect of the thermodiffusive mechanism.

As an example, consider the case of figures 13–15. The vortex pair has the same velocity as in the calculation of §4.1.1 (where quenching was obtained) but its size is smaller ($r/l_F^u = 1.6$ and $u'(r)/s_L^u = 28$). This vortex pair generates a higher strain than the pair used in §4.1.1 but also a higher curvature. Therefore, the Karlovitz number defined by (21) is lower than in the previous sections and reaches a maximum value of 0.6 at a reduced time $t^+ = 0.4$ before it becomes negative after $t^+ = 0.4$ (figure 15). No flame quenching is observed (figure 13). The radius of curvature of the

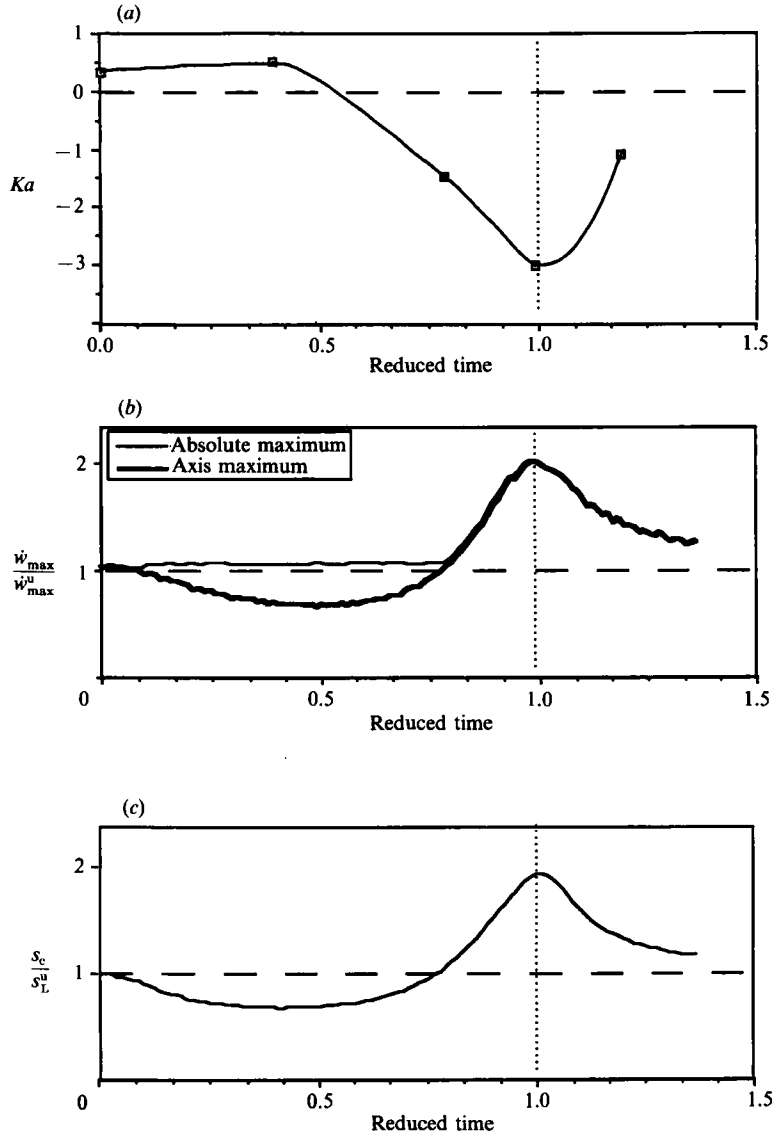

FIGURE 15. (*a*) Karlovitz number, (*b*) maximum reaction rates and (*c*) consumption flame speed on the symmetry axis for an interaction where curvature prevents quenching with $Le = 1.2$ ($r/l^{u}_{F} = 1.6$ and $u'(r)/s^{u}_{L} = 28$).

flame front is of the order of the reaction zone thickness and combustion is notably enhanced on the axis (figure 14). Negative values of the Karlovitz number evaluated on the axis show that the tip of the pocket is compressed instead of being stretched (figure 15). This configuration is, in fact, similar to the flame tip of a Bunsen burner for which it is well known that a Lewis number larger than unity may create high temperatures and large flame speeds (Mizomoto *et al.* 1984; Poinsot *et al.* 1990).

The influence of curvature is not felt during the first instants of the interaction. Between $t^{+} = 0$ and $t^{+} = 0.5$, the flame is affected by the high straining rate and the flame speed on the axis decreases slowly as predicted from asymptotic studies of laminar stagnation point flames (Libby *et al.* 1983). After $t^{+} = 0.5$, the flame front is

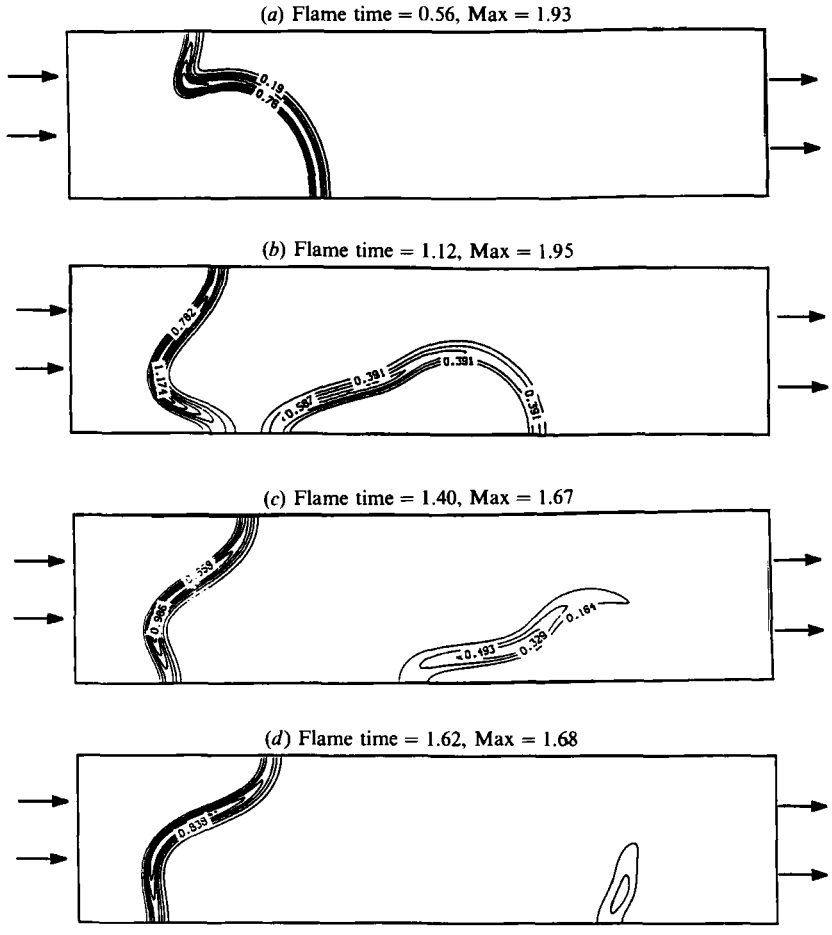

FIGURE 16. Reaction rate fields at four instants for an interaction leading to quenching with $Le = 0.8$ ($r/l_F^u = 3.9$ and $u'(r)/s_L^u = 36$).

sufficiently curved so that the thermo-diffusive effect is stronger than the effect of strain. This yields a negative value of the stretch (figure 15*a*) as well as an increase of the consumption speed on the symmetry axis (figure 15*c*). Furthermore, the vortex pair is being dissipated by viscosity very rapidly because of its small size. At $t^+ = 1$, the maximum vorticity is only 0.02 times its initial value and the maximum reaction rate as well as the flame speed on the axis reach twice their unstretched plane values (figures 15*b* and 15*c*). As a result, the flame front propagates upstream at high speed and progressively relaxes to its original position (figure 13*d*).

The interaction of small vortices with the flame front appears to be dominated by viscous and curvature effects, more than by strain. Note however, that the time variations of the total stretch (which includes strain and curvature term, (21)) are fairly well correlated with the time variations of the consumption flame speed on the symmetry axis for all cases described in this Section (figures 9, 12 and 15). Increasing total flame stretch yields decreased consumption flame speeds. This indicates that the total flame stretch may be a meaningful quantity to correlate the flamelet consumption speeds as a function of the turbulent characteristics. However, the estimation of the flame stretch requires values of strain, displacement speed and

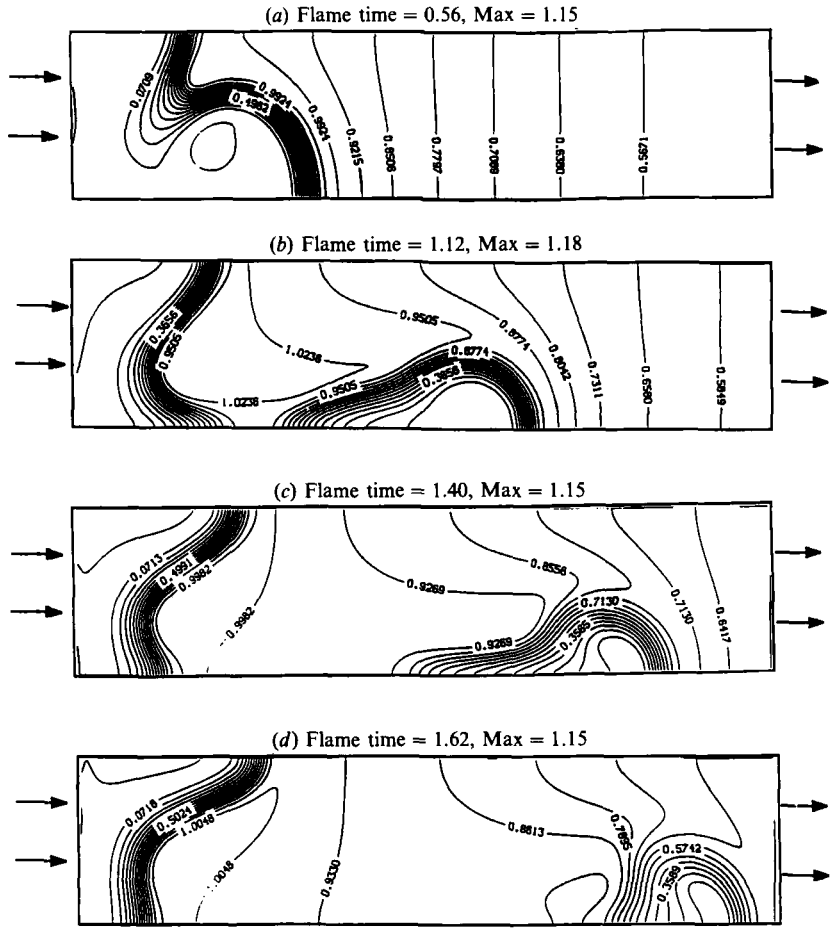

FIGURE 17. Temperature fields at four instants for an interaction leading to quenching with $Le = 0.8$ ($r/l_F^u = 3.9$ and $u'(r)/s_L^u = 36$).

curvature (equation (20)). How to evaluate these quantities from an averaged description of the turbulent flow remains an open question.

4.2. *Flame/vortex interactions for* $Le = 0.8$

The Lewis number used throughout the previous section was 1.2. When the Lewis number is smaller than unity and heat losses are small, flame stretch will increase the flame speed. As confirmed by the experiments of Ishizuka & Law (1982), such flames may be extinguished only by incomplete reaction, for example, by pushing the flame against a solid surface (figure 1). In this case, combustion stops when the flame reaches the solid surface and such phenomena are unlikely to occur in turbulent flames where flame elements move freely to adjust to excessive strain rates. One may then expect that flames with $Le < 1$ may be quenched by stretch only in the presence of significant heat losses. This aspect is now examined by submitting a flame with a Lewis number of 0.8 to the vortex pairs used in §4.1. The heat-loss coefficient is the same as in §4.1.1 ($c = 10^{-4}$) and the diffusion and viscosity coefficients vary with temperature ($b = 0.76$). The speed of this flame is $s_L^u/a = 0.0099$ and its thickness l_F^u is 1.2 times the thickness of the $Le = 1.2$ flame.

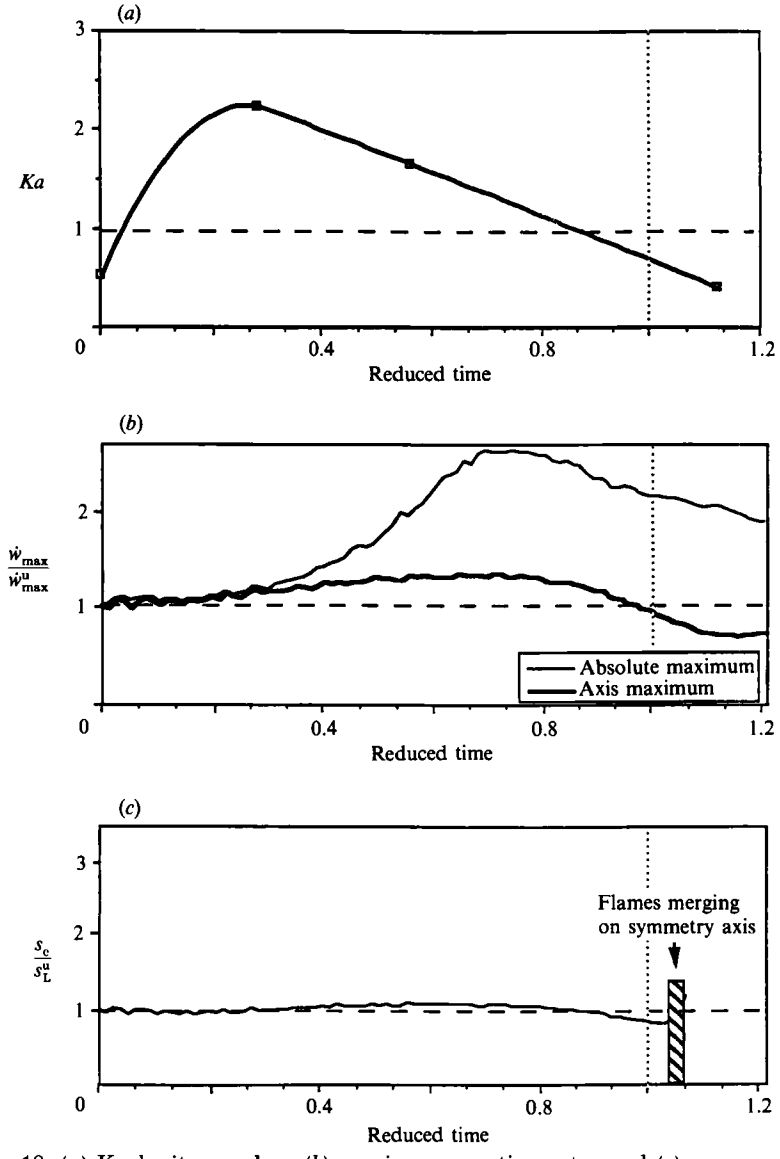

FIGURE 18. (*a*) Karlovitz number, (*b*) maximum reaction rates and (*c*) consumption flame speed on the symmetry axis for an interaction leading to quenching with $Le = 0.8$ ($r/l_F^u = 3.9$ and $u'(r)/s_L^u = 36$).

4.2.1. *Flame quenching by a vortex pair for* $Le = 0.8$

Consider the vortex pair defined in §4.1.1. Because of the lower flame speed and greater flame thickness for $Le = 0.8$, the interaction of this pair with the flame front corresponds to $r/l_F^u = 3.9$ and $u'(r)/s_L^u = 36$. When $Le = 0.8$, this interaction leads again to the formation of a pocket of fresh gases surrounded by a quenched flame front but the flow evolves more rapidly (figures 16–18). The pocket is shed at $t^+ \approx 1$ before quenching takes place (figure 16*b*, *c*). The flame speed on the symmetry axis always remains close to unity (figure 18*c*). The initial flame front structure is recovered before any quenching takes place. This behaviour is due to thermo-diffusive mechanisms which increase the flame speed and the absolute maximum

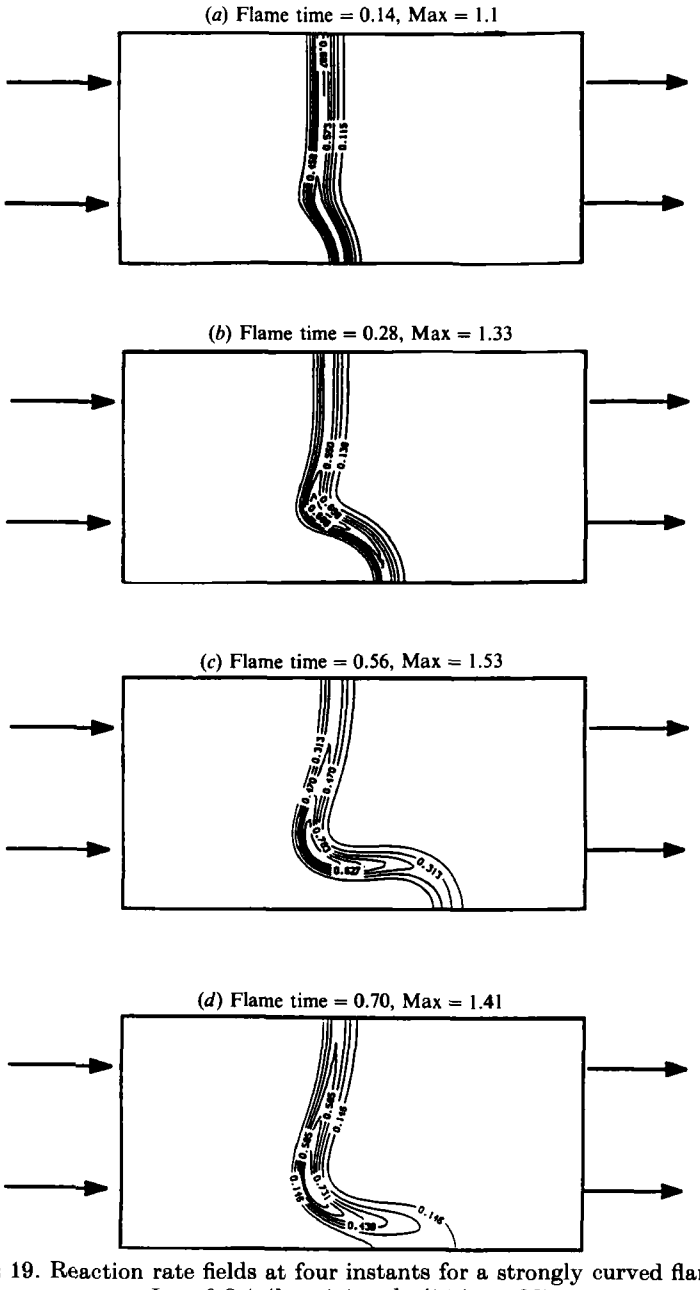

FIGURE 19. Reaction rate fields at four instants for a strongly curved flame with $Le = 0.8$ ($r/l_F^u = 1.4$ and $u'(r)/s_L^u = 36$).

reaction rate (figure 18*b*) on the upstream tails of the flame front and allow these flames to rapidly merge on the axis. However, the pocket of fresh gases is not able to sustain combustion at its tip because of heat losses. The tip is quenched after $t^+ = 1.2$ (figures 16*c* and 17*c*) and the complete pocket border is quenched at time $t^+ = 1.6$ (figures 16*d* and 17*d*). Although the details of the interaction are different for $Le = 1.2$ (figures 7–9) and $Le = 0.8$ (figures 16–18), the overall result is the same and quenching occurs in both cases. Quenching is in this case controlled by heat losses more than by Lewis number effects.

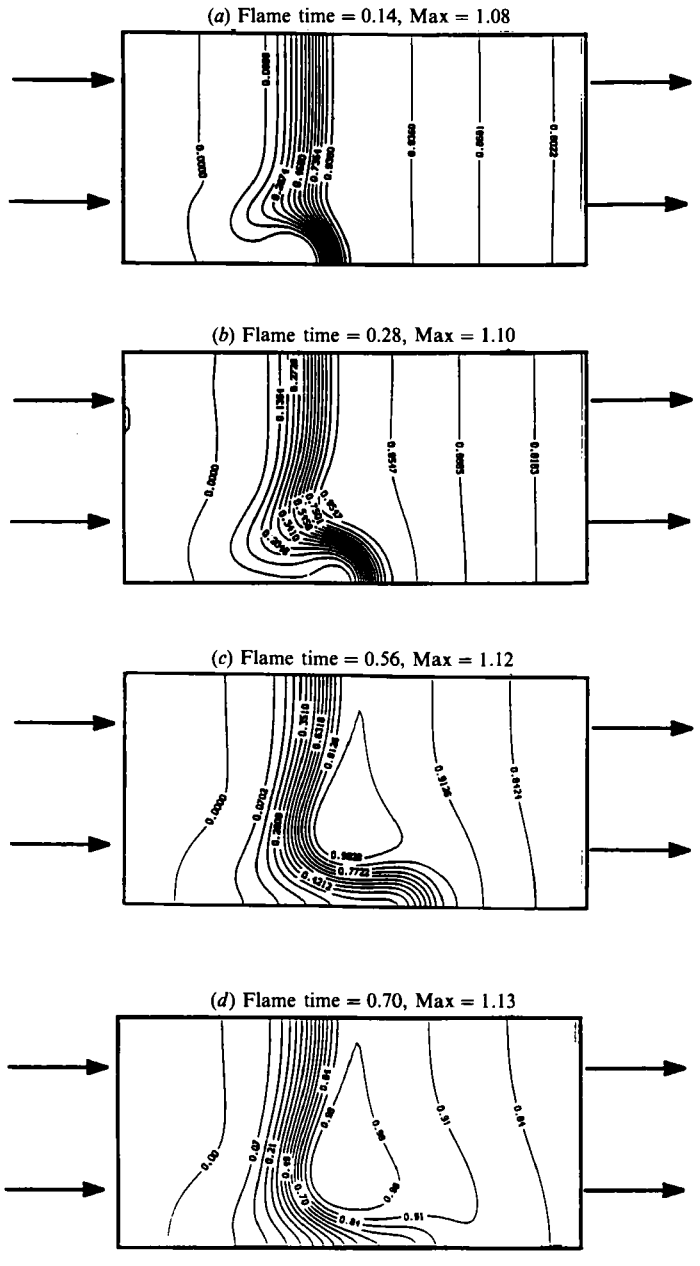

FIGURE 20. Temperature fields at four instants a strongly curved flame with $Le = 0.8$ ($r/l_F^u = 1.4$ and $u'(r)/s_L^u = 36$).

4.2.2. *The effect of curvature and viscosity for* $Le = 0.8$

Flame curvature decreases the flame speed when $Le < 1$. This mechanism is the source of the well-known thermo-diffusive instabilities which lead to the formation of cellular structures in premixed laminar flames (Williams 1985; Clavin & Williams 1982). This fact suggests that small vortices might be able to locally quench a flame front when $Le < 1$. This hypothesis is first tested by computing the interaction between the same vortex pair as in §4.1.2 ($r/l_F^u = 1.4$ and $u'(r)/s_L^u = 36$) and a flame

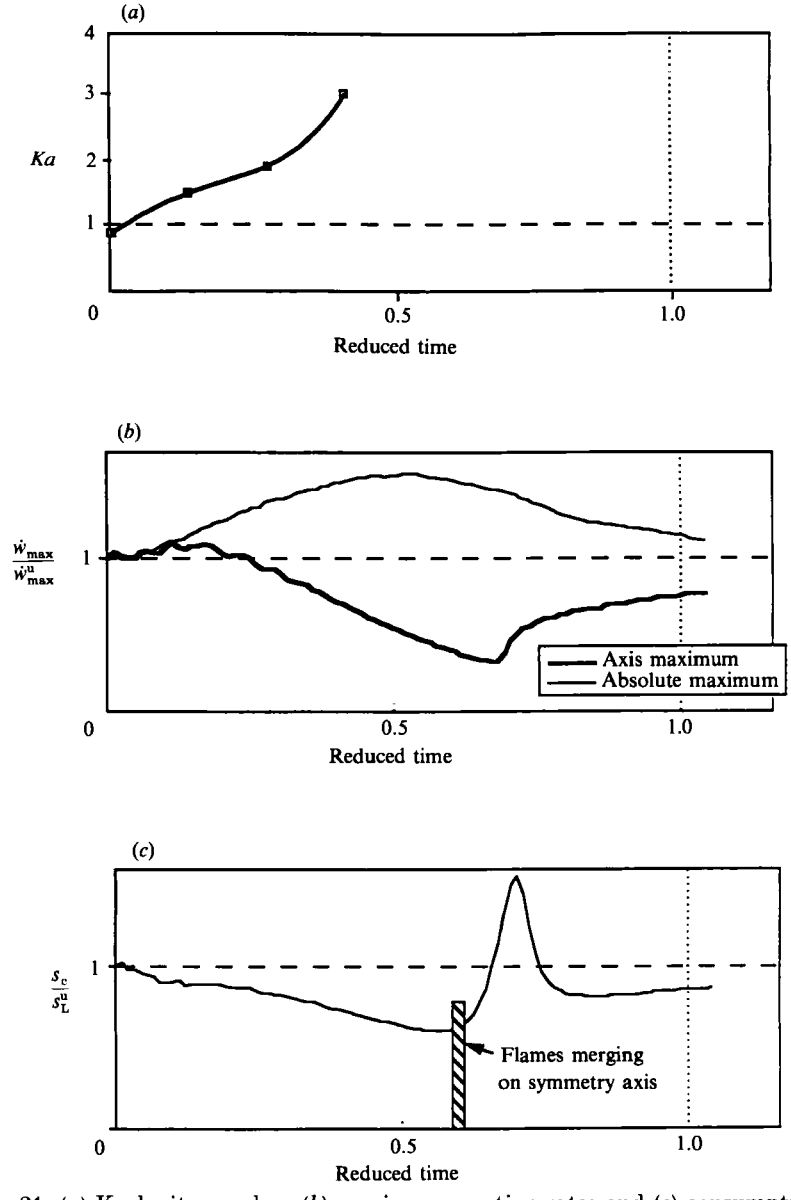

FIGURE 21. (*a*) Karlovitz number, (*b*) maximum reaction rates and (*c*) consumption flame speed on the symmetry axis for a strongly curved flame with $Le = 0.8$ ($r/l^{u}_{F} = 1.4$ and $u'(r)/s^{u}_{L} = 36$).

with $Le = 0.8$. Results are displayed in figures 19–21. While this configuration confirms the expected trend (the flame speed is decreased on the axis to a value of $0.6s^{u}_{L}$ (figure 21*c*)), no quenching occurs (figure 19). As in the previous case, thermo-diffusive mechanisms increase notably the flame speeds of the left-most elements of the flame. The absolute maximum of the reaction rate is obtained at these locations and reaches $1.7\dot{w}^{u}_{max}$ (figure 21*b*). While the tip of the flame is highly curved and starts being quenched (figure 20*c*), the flame front elements located on the sides of the structure propagate at high speed towards the axis. This leads to a complete consumption of the pocket of fresh gases before any quenching may take place. The interaction proceeds at a fast pace and is over after less than one flame time. The

Karlovitz number (figure 21*a*) is not computed at $t^+ = 0.4$ because the flame structure is too thick compared to the flow scales to yield a meaningful expression of the total stretch (equation (20)).

If a smaller vortex is used to increase the effects of curvature, the power of the vortex $P(r) = (r/l_F^u)^2$ is decreased and simulations show that the resultant vorticity field is rapidly dissipated by viscosity. If the vortex rotation speed is increased, the stretch induced on the flame front also increases and enhances the flame speed on the axis. Different configurations were also tried in which the vortices were turning in the opposite direction and were compressing the flame front. In this case, their self-induced velocity pushes the pair upstream, away from the flame front. Altogether, no quenching by small vortices was obtained when $Le = 0.8$. Once more, as far as quenching is concerned, this conclusion is similar to that obtained for $Le = 1.2$. However, the processes governing flame/vortex interactions for $Le = 1.2$ and 0.8 are different. For $Le = 1.2$, because of curvature, the flame speed at the tip of the pocket increased by a factor of two (figure 15), preventing any quenching and bringing the flame front back to its initial planar shape. For $Le = 0.8$, the flame speed at the tip of the pocket decreases with time (figure 21). The reason why quenching does not occur in this situation is the high consumption speeds on the tails of the flame (due to thermo-diffusive mechanisms) which lead to a collapse of the structure when the tails merge on the symmetry axis.

5. The spectral diagram and the new turbulent combustion diagram

5.1. *The spectral diagram for* $Le = 1.2$

We have examined in §4 different examples of interaction between a vortex pair and a laminar flame front. Depending on the scale r and on the vortex pair maximum velocity $u'(r)$, the calculations indicate that the interaction may lead to different results: a local quenching of the front (with or without pocket formation); the formation of a pocket of fresh gases in the burnt gases without quenching; a wrinkled flame front; a negligible global effect without noticeable flame wrinkling or thickening.

These results are summarized in the spectral diagram of figure 22. Points 1, 2 and 3 correspond respectively, to the flame quenching case (§4.1.1), the pocket formation case (§4.1.2) and the curved flame case (§4.1.3). The diagram was plotted for $Le = 1.2$ (owing to the high value of heat losses used in this work, the effect of Lewis number is weak and the diagram for $Le = 0.8$ would be very close to the one presented in figure 22 for $Le = 1.2$.)

Two curves are also plotted in this diagram. (i) The quenching curve distinguishes vortices which locally quench the flame front. It is fitted to the data points for $0.81 < r/l_F^u < 11$ and extended for large vortex sizes $r/l_F^u > 11$ to match the line $Ka(r) = (u'(r)/r)/(s_L^u/l_F^u) = 1$. This asymptotic procedure is adopted because large vortices stretch the flame front as in a stagnation-point flow. The strain rate is sustained for long times and little curvature is induced. Therefore, quenching by large structures is only determined by the ratio of vortex-induced stretch to critical flame stretch and occurs when $Ka(r) = 1$. (ii) The cutoff limit corresponds to vortices which induce a maximum modification of the total reaction rate of 5%. No calculations were performed for $r/l_F^u > 5$ so that the position of the cutoff limit in this region is uncertain.

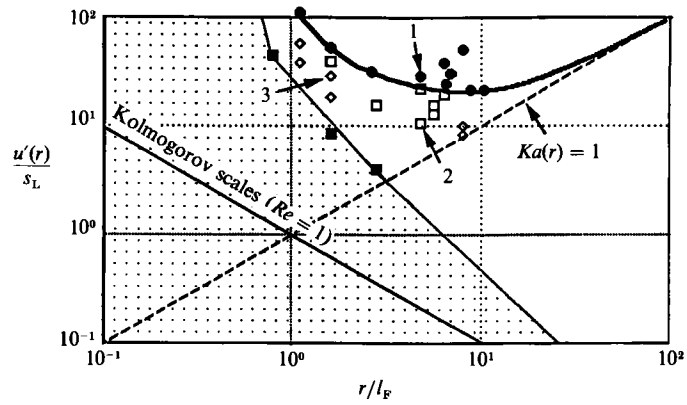

FIGURE 22. Spectral diagram deduced from direct simulations for $Le = 1.2$, $b = 0.76$, $c = 0.0001$, $\alpha = 0.75$ and $\beta = 8$. ●, Quenching; □, pockets; ◇, wrinkled; ■, no effects; ——, cutoff limit; ——, quenching limit.

5.2. *Construction of the premixed turbulent combustion diagram*

The spectral diagram displayed in figure 22 may be used to deduce a premixed turbulent combustion diagram under the following assumptions: (i) turbulence in the fresh gases follows the Kolmogorov relation $u'(r)^3/r = \epsilon$; (ii) a single vortex structure interacts at a given time with the flame front; (iii) any turbulent structure located in the quenching zone of the spectral diagram will locally quench the flame front and induce a distributed reaction regime.

These assumptions are rather crude. For example, it is clear that turbulent scales in the quenching zone will not quench the flame front if the energy density corresponding to these scales is too low. Therefore assumption (iii) is probably not satisfied. A more precise approach would consist in introducing a probability density function (p.d.f.) for the different scales or for the strain rates they impose on the flame front (Cant & Bray 1988; Abdel-Gayed, Bradley & Lau 1988; Meneveau & Poinsot 1991). However, to first order, it is reasonable to assume that the existence of one structure able to quench the flame front is sufficient to lead to a partially quenched flame front (even though this structure might not be statistically present at all times). This hypothesis leads to a 'maximum quenching' interaction diagram. More complex criterions for quenching are derived in Meneveau & Poinsot (1991).

Another important limitation of the present approach is also found in the range of small and energetic scales. In this case, the interaction between many small vortices and the flame front is difficult to assess from the behaviour of a single vortex pair. A study of the well-stirred combustion regime would therefore require a simulation of a complete turbulent reacting flow.

Under the previous assumptions, constructing the turbulent combustion diagram is straightforward. A turbulent field of type B (figure 23) will contain scales which will act on the flame front in different ways: eddies whose sizes are between the Kolmogorov scale and the cutoff scale (dashed line) will be inefficient and will not affect the flame front at all. Vortices larger than the cutoff scale (solid line) will be able to affect the flame front, to wrinkle it or to form pockets but be unable to induce local quenching. Point B with therefore correspond to an extended flamelet regime. In the case of field A, even the integral scale will lack the energy to interact with the flame front and the latter will remain pseudo-laminar. Turbulent field C contains scales that are capable of locally quenching the flame front (double-width solid line).

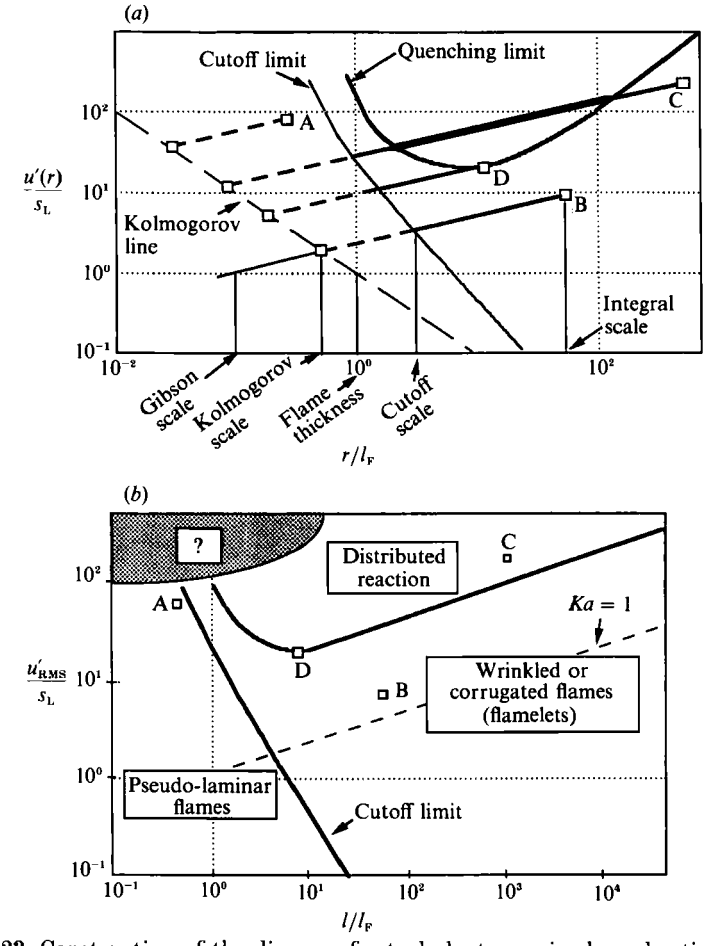

FIGURE 23. Construction of the diagram for turbulent premixed combustion (*b*) using the spectral diagram (*a*) for $Le = 1.2$, $b = 0.76$ and $c = 0.0001$.

Note that these scales are larger and faster by orders of magnitude than the Kolmogorov scale η, while the Klimov–Williams approach assumes that eddies of size η are able to induce flame quenching. Type C turbulence will correspond to a distributed reaction regime. The distributed reaction regime limit is obtained by taking the tangent with a slope of $\frac{1}{3}$ to the quenching limit of the spectral diagram. Comparing this diagram (figure 23*b*) with the standard turbulent combustion diagram (figure 3*a*) reveals that the domain where distributed reaction sheets may be expected has moved at least an order of magnitude towards more intense fields.

It is possible now to discuss further the influence of the heat losses. The value of the heat-loss coefficient used in this study is high enough to consider it as a maximum in most practical flames. Therefore real flames will exhibit less quenching and the spectral diagram, as well as the final turbulent combustion diagram, will move towards more intense fields as shown in figure 24. The limit of the extended flamelet regime is dependent on heat losses but in all cases, the domain of applicability of flamelet modelling will be much larger than expected from classical turbulent combustion diagrams. Moreover, flames with low heat losses and a Lewis number lower than unity will be very difficult to quench and might always be in an extended flamelet regime.

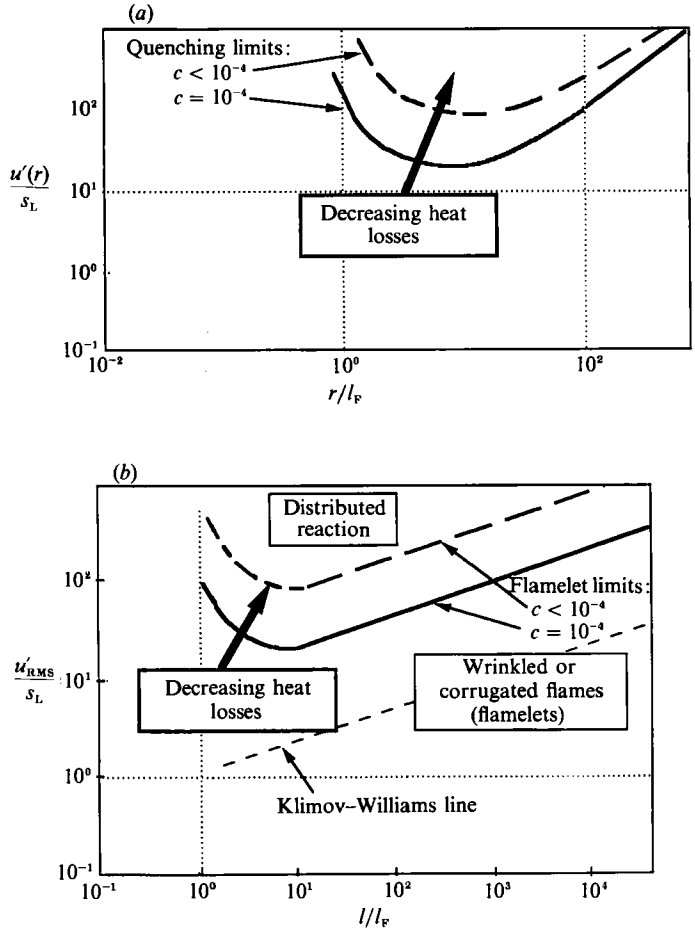

FIGURE 24. Evolution of the spectral diagram (*a*) and of the diagram for turbulent premixed combustion (*b*) when the heat-loss coefficient is changing (for $Le = 1.2$, $b = 0.76$).

5.3. *Characteristic scales in premixed turbulent combustion*

Different characteristic scales may be extracted from the spectral diagram (figure 23*a*): the cutoff scale and the quenching scale.

The cutoff scale l_{cutoff} is obtained at the intersection of the turbulence line with the cutoff limit. It corresponds to the smallest scale that may influence the reaction rate in a noticeable way. It is the length that should be used in a fractal estimate of the flame area. Its value is determined mainly by viscous and thermo-diffusive effects and not by heat-loss mechanisms. A best fit derived from the calculations is

$$\frac{l_{\text{cutoff}}}{l_F^u} = 0.2 + 5.5/\epsilon^{+\frac{1}{6}}, \tag{22}$$

where $\epsilon^+ = \epsilon l_F^u / s_L^{u3}$ is the reduced dissipation rate. Note that the Kolmogorov scale η is

$$\eta/l_F^u = 1/\epsilon^{+\frac{1}{4}}, \tag{23}$$

The cutoff scale may also be expressed in terms of the Kolmogorov scale η and the integral Reynolds number Re_l by

$$\frac{l_{\text{cutoff}}}{\eta} = \frac{0.74}{Re_l^{\frac{1}{4}}}\frac{u'}{s_{\text{L}}^{\text{u}}} + \frac{16.3}{Re_l^{\frac{1}{2}}}\left(\frac{u'}{s_{\text{L}}^{\text{u}}}\right)^{\frac{1}{3}}. \tag{24}$$

Note that the derivation of (24) from (22) is done by using $s_{\text{L}}^{\text{u}} l_{\text{F}}^{\text{u}}/\nu = 3.7$.

The cutoff scale is always larger than $0.2 l_{\text{F}}^{\text{u}}$ (see (22)). It is also larger than the Kolmogorov scale η even when η is larger than the flame front thickness l_{F}. Kolmogorov scales do not carry enough energy to affect the flame front in any situation. These results are in agreement with the experiments of Shepherd, Cheng & Goix (1989) showing that the cutoff scale in premixed turbulent stagnation-point flames is much larger than the Kolmogorov scale.

Other expressions for cutoff scales may be found in the literature (Peters 1986; Gouldin *et al.* 1989). The well-known Gibson scale l_{G} proposed by Peters (1986) is defined by $l_{\text{G}} = s_{\text{L}}^{\text{u}3}/\epsilon$ or

$$l_{\text{G}}/l_{\text{F}}^{\text{u}} = 1/\epsilon^{+}. \tag{25}$$

Figure 23(*a*) shows all relevant scales (l_{G}, η, l_{F}, l_{cutoff} and l) in a case without quenching where $\epsilon^{+} > 1$ (case B in figure 23*a*). The Gibson scale l_{G} is lower than the Kolmogorov scale η and does not constitute a physically meaningful quantity in this case.

The difference between the arguments used by Peters to derive the Gibson scale and the present analysis comes from the fact that Peters assumes that a given vortex will interact efficiently with the flame front when its velocity is equal to the flame speed. This assumption neglects essential effects related to the vortex/flame interaction such as dissipation of small vortices by viscosity and the influence of transient dynamics and curvature. Although the Gibson scale might give better results for lower turbulence intensities, expression (22) appears to be more physically meaningful in most cases. The determination of the cutoff scale is important for many approaches of premixed turbulent combustion and experiments with high spatial resolution would be needed to allow comparisons with model predictions.

The quenching scales are the cross-points between the turbulence line and the quenching limit. They represent the sizes of the smallest and largest vortices which are able to locally quench the flame front (figure 23*a*). The existence of two scale limits for quenching is an interesting outcome of the analysis. Large vortices will not quench the flame front because their stretch is too small ($Ka(r) < 1$). On the other end of the spectrum, small scales will also be unable to quench the flame because their power is too small or because they create strongly curved flames (both effects are characterized by $P(r) < 1$).

While the cutoff scale may be defined in each case, the quenching scales do not exist for all turbulent fields. Turbulent field D in figure 23(*a*) corresponds to the minimum turbulence intensity for quenching. This leads to a simple quenching criterion:

$$\epsilon^{+} = \frac{(u'/s_{\text{L}}^{\text{u}})^3}{l/l_{\text{F}}^{\text{u}}} > 10^3 \quad \text{or} \quad u'/s_{\text{L}}^{\text{u}} > 4 Re_l^{0.25} \tag{26}$$

and

$$Re_l = u' l/\nu > 250. \tag{27}$$

Equations (26) and (27) set minimum values for quenching on the reduced dissipation rate ϵ^{+} and on the Reynolds number Re_l respectively. These correlations

may be compared with the experimental relations established by Abdel-Gayed & Bradley (1989) in a study of quenching of premixed flames in fan-stirred bombs. These authors indicate that for $Re_l > 300$, partial quenching occurs when $u'/s_L^u > 2Re_l^{0.25}$ and total flame quenching for $u'/s_L^u > 3Re_l^{0.25}$. While heat losses are certainly present in the experiment, their influence was not documented. Therefore, although condition (26) gives the same functional dependence as Abdel-Gayed & Bradley's results, the values of the proportionality coefficient (4 for direct simulation, 2 or 3 for experimental results) are difficult to compare. For values of Re_l lower than 300, quenching is still obtained in experiments but the data cannot be correlated using a functional dependence similar to (26). Our results suggest that quenching for $Re_l < 300$ is not due to stretch, for which we find a lower limit of $Re_l = 250$, but more probably to purely thermal processes. However, quenching scales are strong functions of heat losses and more experimental results correlating heat losses with quenching in premixed turbulent flames would be needed to assess this point.

6. Conclusion

This paper presents new results on some fundamental mechanisms governing premixed turbulent combustion. The analysis includes curvature, viscous and transient effects as well as a simple model for volumetric heat losses. It uses direct simulation to describe the interaction between a flame and a vortex pattern.

The variations of the consumption speed of flamelets and the existence of quenching in premixed turbulent flames are investigated by studying the interaction of a vortex pair with a laminar flame front. Most flamelet models assume that (i) quenching in a turbulent premixed flame is controlled by stretch and that (ii) strain alone may be used to evaluate stretch. Therefore, quenching in turbulent flames is studied like quenching in a planar stagnation-point flame. However, laminar stagnation-point flames are planar and submitted to a constant stretch while flame elements in a turbulent flame are curved and submitted to variable stretch.

For a Lewis number of 1.2 and strong heat losses, the present results show that the analogy between turbulent flame elements of size r and stagnation-point flames is valid for large vortices (typically $r/l_F^u > 5$ if r is the vortex pair size and l_F^u is the unstretched laminar flame thickness). These large structures may quench a flame front if the strain they induce on the flamc is larger than the critical strain for extinction of a stagnation point flame ($Ka(r) = [u'(r)/r]/[s_L^u/l_F^u] > 1$). However, the interaction between small vortices ($r/l_F^u < 5$) and a flame front is controlled by curvature and viscous effects more than by strain. Very small vortices ($r/l_F^u < 0.5$) are dissipated by viscosity too rapidly to influence the flame front significantly. Vortices whose size is of the order of the flame front thickness ($r/l_F^u \approx 0.5$ to 5) induce high curvatures which prevent quenching because thermo-diffusive mechanisms counteract the influence of strain. The first implication of these results for flamelet modelling of premixed turbulent combustion is that planar laminar stagnation-point flames are correct models for turbulent flamelets only when the radius of curvature of the turbulent flame front is larger than five times the laminar unstrained flame thickness ($r/l_F^u > 5$) and stretch is controlled by strain only (not by curvature). Below this limit (when $r/l_F^u < 5$), planar laminar stagnation-point flames cannot be accurate prototypes of flamelets because they do not take into account curvature, viscous and time-dependent effects. Flamelet models may still be adequate in this case but they will have to include at least curvature effects to describe the dynamical behaviour of individual flamelets. It is worth indicating that the variations of the *total stretch*

(which includes strain and curvature effects) correlate fairly well with the changes of the consumption speed of the flame front. This result is similar to conclusions obtained from asymptotic studies (Clavin & Joulin 1983) but it raises a major difficulty when turbulent flames are concerned because an estimate of the flamelets' curvature has to be deduced from averaged descriptions of the reacting flow. Flamelet models usually estimate strain from simple arguments based on dimensional analysis. Estimating curvature is a more difficult task (Pope 1988; Candel & Poinsot 1990) and the practical implication of flamelet models using strain and curvature remains an open question.

As far as models are concerned, this result suggests that the laminar flamelet assumption, which assumes that the structure of flamelets in a turbulent flame is similar to the structure of laminar planar stagnation-point flames, is probably never rigorously satisfied. An extended flamelet definition is therefore proposed: a turbulent flame is in a flamelet regime if fresh and burnt gases are always separated by a thin reacting interface, even though this interface may not have an exactly laminar-like flame structure. This extended definition still allows practical models to be derived and corresponds to a more realistic application of flamelet concepts.

The effect of the Lewis number was investigated by considering a flame with $Le = 0.8$. Thermo-diffusive instabilities have important effects when Le is less than 1. While the detailed interaction mechanisms for $Le = 0.8$ and $Le = 1.2$ flames are different, the quenching characteristics are unchanged because the process is mainly controlled by heat losses. The case of flames with $Le < 1$ and small heat losses remains and open question but one may expect that such flames will be difficult to extinguish.

When quenching takes place, a pocket of unburnt mixture may cross the flame front without burning, leading to mixing of fresh unburnt gases with burnt gases (cooled by heat losses) without combustion. Although the subsequent evolution of the reacting flow was not investigated here, such a quenching event is likely to indicate the transition between a flamelet regime and a distributed reaction regime. Therefore, results obtained for the interaction of an isolated vortex pair with a flame front may be used to deduce the response of a flame element to a turbulent flow. For a Lewis number of 1.2 and strong heat losses ($c = 10^{-4}$), direct simulation results yield a spectral diagram describing the interaction between an isolated vortex pair and a flame front. Assuming that vortex pairs are the most efficient structures which may induce flame quenching, the spectral diagram may be employed to define a modified premixed turbulent combustion diagram. Results show that classical diagrams underestimate the resistance of flame fronts to turbulent eddies, mainly because they neglect viscous, transient and curvature effects. These effects are especially important when small scales are considered. The vortices that may quench a flame front are orders of magnitude larger and faster than Kolmogorov scales.

The Klimov–Williams criterion for flamelet regimes may be reassessed on this basis. The domain in which extended flamelet regimes are expected appears to be larger than usually accepted for laminar flamelet regimes. In fact, the boundaries of the laminar flamelet regime itself appear to be quite imprecise and direct simulations (Haworth & Poinsot 1990; Rutland & Trouvé 1990) as well as experimental evidence (Katsuki *et al.* 1990) suggest that flamelets might preserve a laminar-like structure even when the Kolmogorov scale is smaller than the flame thickness. This would mean that, from an engineering point of view, the laminar and the extended flamelet regimes would not be very different. It does not imply, however, that planar laminar flames are good prototypes for flamelets neither in the extended flamelet

approximation, nor in the laminar one: as indicated above, curvature and transient effects should be included in all flamelet models.

The upper boundary of the extended flamelet regime is a strong function of the heat-loss coefficient. In most practical cases, heat losses are certainly smaller than in the present work and extended flamelet models for premixed turbulent combustion probably have a broader applicability than previously thought.

Characteristic scales may be extracted from the spectral diagram. A cutoff scale scale indicating the size of the smallest eddy interacting efficiently with the flame front is derived. This scale is affected mainly by viscous and thermo-diffusive mechanisms. It is a fundamental quantity in the fractal analysis of turbulent combustion but also for flamelet models in general because it fixed the size of the smallest scales that may wrinkle the flame front. The cutoff scale is always larger than the Kolmogorov scale. In very intense turbulent fields, it may be of the order of the flame front thickness.

Quenching criteria are also obtained. It is shown that quenching by a vortex pair only occurs within a limited range of scales. The lifetime of small vortices is too short to allow a strong interaction with the flame. At the other end of the turbulence spectrum, large vortices induce a flame stretch that is too low to cause flame quenching. For the case considered in this paper ($Le = 1.2$ and $c = 10^{-4}$), no quenching is obtained if the integral Reynolds number $Re_l = u'l/\nu$ is less than 300. When $Re_l > 300$, a quenching condition correlating the turbulence intensity u' (normalized by the laminar flame speed s_L^u) and the Reynolds number Re_l is obtained and corresponds fairly well to experimental results of Abdel-Gayed & Bradley (1989). Heat losses, however, are mainly responsible for flame quenching and their importance is not usually documented in experimental studies to allow precise comparisons. More generally, it is shown that direct simulations provide remarkable new insights in the processes which govern turbulent combustion.

The first author would like to thank Professor T. Bowman, Professor J. Ferziger, Professor R. Dibble, Dr A. Trouvé, Dr D. Haworth, Professor S. Mahalingam and Professor C. Rutland for many helpful discussions. We all wish to thank the reviewers for their careful criticism of this article and for many suggestions now incorporated in the text. This study was supported by the Center for Turbulence Research.

REFERENCES

ABDEL-GAYED, R. G. & BRADLEY, D. 1985 Criteria for turbulent propagation limits of premixed flames. *Combust. Flame* **62**, 61.

ABDEL-GAYED, R. G. & BRADLEY, D. 1989 combustion regimes and the straining of turbulent premixed flames. *Combust. Flame* **76**, 213.

ABDEL-GAYED, R. G., BRADLEY, D. & LAW, A. K. C. 1988 The straining of premixed turbulent flames. *Twenty Second Symp. (Intl) on Combustion*, p. 731. The Combustion Institute.

ASHURST, W. T., PETERS, N. & SMOOKE, M. D. 1987 Numerical simulation of turbulent flame structure with non-unity Lewis number. *Combust. Sci. Tech.* **53**, 339.

BABIANO, A., BASDEVANT, C., LEGRAS, B. & SADOURNY, R. 1987 Vorticity and passive-scalar dynamics in two-dimensional turbulence. *J. Fluid Mech.* **183**, 379.

BARRÈRE, M. 1974 Modèles de combustion. *Revue Gén. Thermique* **148**, 295.

BASDEVANT, C., COUDER, Y. & SADOURNY, R. 1985. Vortices and vortex couples in two-dimensional turbulence. In *Macroscopic Modelling of Turbulent Flows*. Lecture notes in Physics, Vol. 230, p. 327. Springer.

BEER, J. M. & CHIGIER, N. A. 1983 In *Combustion Aerodynamics*. p. 61. Malabar, Florida: Krieger.

BORGHI, R. 1985 On the structure and morphology of turbulent premixed flames. In *Recent Advances in Aerospace Science* (ed. C. Bruno & C. Casci), p. 117. Plenum.

BORGHI, R. 1988 Turbulent combustion modelling. *Prog. Energy Combust. Sci.* **14**, 245–292.

BRAY, K. N. C. 1980 Turbulent flows with premixed reactants in turbulent reacting flows. In *Topics in Applied Physics* (ed. P. A. Libby & F. A. Williams), vol. 44, p. 115. Springer.

BRAY, K. N. C. 1987 Methods on including realistic chemical reaction mechanisms in turbulent combustion models. In *Complex Chemical Reactions* (ed. J. Warnatz & W. Jager), vol. 41, p. 356. Springer.

BRAY, K. N. C. & LIBBY, P. 1986 Passage times and flamelet crossing frequencies in premixed turbulent combustion. *Combust. Sci. Tech.* **47**, 253.

BUSH, W. & FENDELL, F. 1970 Asymptotic analysis of laminar flame propagation for general Lewis numbers. *Combust. Sci. Tech.* **1**, 421.

CANDEL, S. & POINSOT, T. 1990 Flame stretch and the balance equation for the flame area. *Combust. Sci. Tech.* **70**, 1.

CANDEL, S., VEYNANTE, D., LACAS, F., MAISTRET, E., DARABIHA, N. & POINSOT, T. 1990 Coherent flame model: applications and recent extensions. *Recent Advances in Combustion Modelling* (ed. B. Larrouturou). World Scientific.

CANT, R. & BRAY, K. 1988 Strained laminar flamelet calculations of premixed turbulent combustion in a closed vessel. *Twenty Second Symp. (Intl) on Combustion*, p. 791. The Combustion Institute.

CANT, R. & RUTLAND, C. 1990 Statistics for laminar flamelet modelling. *Proc. Summer Program of the Center for Turbulence Research*. Stanford University.

CARRIER, G., FENDELL, F. & MARBLE, F. 1975 The effect of strain rate on diffusion flames. *SIAM J. Appl. Math.* **28**, 463.

CATTOLICA, R. & VOSEN, S. 1987 Combustion-torch ignition: fluorescence imaging of OH concentration. *Combust. Flame* **68**, 267.

CETEGEN, B. & SIRIGNANO, W. 1988 *AIAA Paper* 88-0730.

CHENG, R., SHEPHERD, I. & TALBOT, L. 1988 Reaction rates in premixed turbulent flames and their relevance to the turbulent burning speed. *Twenty Second Symp. (Intl) on Combustion*, p. 771. The Combustion Institute.

CLAVIN, P. & JOULIN, G. 1983 Premixed flames in large scale and high intensity turbulent flow. *J. Phys. Lett.* **44**, L1.

CLAVIN, P. & WILLIAMS, F. 1982 Effects of molecular diffusion and of thermal expansion on the structure and dynamics of premixed flames in turbulent flows of large scale and low intensity. *J. Fluid Mech.* **116**, 251.

DAMKÖHLER, G. 1940 Der Einfluß der Turbulenz auf die Flammenge-schwindigkeit in Gasgemischen. *Z. Elektrochem.* **46**, 601.

DARABIHA, N., CANDEL, S. & MARBLE, F. 1986 The effect of strain rate on a premixed laminar flame. *Combust. Flame* **64**, 203.

DARABIHA, N., GIOVANGIGLI, V., TROUVE, A., CANDEL, S. & ESPOSITO, E. 1989 Coherent flame description of turbulent premixed flames. *Proc. French-USA Workshop on Turbulent Combustion* (ed. R. Borghi & S. Murthy). Springer.

FARGE, M. & SADOURNY, R. 1989 Wave-vortex dynamics in rotating shallow water. *J. Fluid Mech.* **206**, 433.

GHONIEM, A. & KRISHNAN, A. 1988 Origin and manifestation of flow-combustion interactions in a premixed shear layer. *Twenty Second Symp. (Int) on Combustion*, p. 665. The Combustion Institute.

GIOVANGIGLI, V. & SMOOKE, M. 1987 Extinction of strained premixed laminar flames with complex chemistry. *Combust. Sci. & Tech.* **53**, 23.

GOULDIN, F., BRAY, K. & CHEN, J.-Y. 1989 Chemical closure model for fractal flamelets. *Combust. Flam* **77**, 241.

HAWORTH, D., DRAKE, M., POPE, S. & BLINT, R. 1988 The importance of time-dependent flame structures in stretched laminar flamelet models for turbulent jet diffusion flames. *Twenty Second Symp. (Intl) on Combustion*. The Combustion Institute.

HAWORTH, D. & POINSOT, T. 1990 The influence of non-unity Lewis number and non homogeneous mixture in premixed turbulent combustion. *Proc. Summer Program of the Center for Turbulence Research, Stanford University.*

ISHIZUKA, S. & LAW, C. K. 1982 An experimental study on extinction of stretched premixed flames. *Nineteenth Symp. (Intl) on Combustion*, p. 327. The Combustion Institute.

JAROSINSKI, J., LEE, J. & KNYSTAUTAS, R. 1988 Interaction of a vortex ring and a laminar flame. *Twenty Second Symp. (Intl) on Combustion*, p. 505. The Combustion Institute.

JOU, W.-H. & RILEY, J. 1989 Progress in direct numerical simulation of turbulent reacting flows. *AIAA J.* **27**, 1543.

KARAGOZIAN, A. & MARBLE, F. E. 1986 Study of a diffusion flame in a stretched vortex. *Combust. Sci. Tech.* **45**, 65.

KATSUKI, M., MIZUTANI, Y., YASUDA, T., KUROSAWA, Y., KOBAYASHI, K. & TAKAHASHI, T. 1990 Local fine flame structure and its influence on mixing processes in turbulent premixed flames. *Combust. Flame* **82**, 93.

LAVERDANT, A. & CANDEL, S. 1989 combustion of diffusion and premixed flames rolled-up in vortex structures. *AIAA J. Propulsion and Power* **5**, 134.

LAW, C. K., ZHU, D. L. & YU, G. 1986 Propagation and extinction of stretched premixed flames. *Twenty First Symp. (Intl) on Combustion*, p. 1419. The Combustion Institute.

LELE, S. 1989 Direct numerical simulation of compressible shear flows. *AIAA Paper* 89-0374.

LELE, S. 1991 Compact finite difference schemes with spectral-like resolution. *J. Comput. Phys.* (submitted).

LEWIS, B. & VON ELBE, G. 1987 In *Combustion, Flames and Explosions of Gases* (3rd edn). Academic.

LIBBY, P., LIÑÀN, A. & WILLIAMS, F. 1983 Strained premixed laminar flames with non-unity Lewis number. *Combust. Sci. Tech.* **34**, 257.

LIBBY, P. & WILLIAMS, F. 1982 Structure of laminar flamelets in premixed turbulent flames. *Combust. Flame* **44**, 287.

LIBBY, P. & WILLIAMS, F. 1987 Premixed flames with general rates of strain. *Combust. Sci. Tech.* **54**, 237.

MANTZARAS, J., FELTON, P. & BRACCO, F. 1989 Fractals and turbulent premixed engine flames. *Combust. Flame* **77**, 295.

MARBLE, F. E. 1985 Growth of a diffusion flame in the field of a vortex. In *Recent Advances in Aerospace Science* (ed. C. Bruno & C. Casci), p. 395. Plenum.

MARBLE, F. E. & BROADWELL, J. 1977 The coherent flame model for turbulent chemical reactions. *Project SQUID, Rep.* TRW-9-PU.

MATALON, M. 1983 On flame stretch. *Combust. Sci. Tech.* **31**, 169.

MENEVEAU, C. & POINSOT, T. 1991 Stretching and quenching of flamelets in premixed turbulent combustion. *Combust. Flame* (to appear).

MIKOLAITIS, D. 1984*a* The interaction of flame curvature and stretch, Part 1: the concave premixed flame. *Combust. Flame* **57**, 25.

MIKOLAITIS, D. 1984*b* The interaction of flame curvature and stretch, Part 2: the convex premixed flame. *Combust. Flame* **58**, 23.

MIZOMOTO, M., ASAKA, Y., IKAI, S. & LAW, C. K. 1984 Effects of preferential diffusion on the burning intensity of curved flames. *Twentieth Symp. (Intl) on Combustion*, p. 1933. The Combustion Institute.

PELCE, P. & CLAVIN, P. 1982 Influence of hydrodynamics and diffusion upon the stability limits of laminar premixed flames. *J. Fluid Mech.* **124**, 219.

PETERS, N. 1986 Laminar flamelet concepts in turbulent combustion. *Twenty First Symp. (Intl) on Combustion*, p. 1231. The Combustion Institute.

POINSOT, T., ECHEKKI, T. & MUNGAL, G. 1990 Curved flame propagation in non-uniform flows: from the flame tip of Bunsen burners to turbulent combustion. *Combust. Sci. and Tech.* (submitted).

POINSOT, T. & LELE, S. 1991 Boundary conditions for direct simulations of compressible viscous flows. *J. Comput. Phys* (submitted).

POPE, S. 1988 The evolution of surfaces in turbulence. *Intl J. Engng Sci.* **26**, 445.

POPE, S. & CHENG, W. 1988 The stochastic flamelet model of turbulent premixed combustion. *Twenty Second Symp. (Intl) on Combustion*, p. 781. The Combustion Institute.

RUTLAND, C. J. 1989 Effect of strain, vorticity and turbulence on premixed flames. Ph.D. Thesis, Stanford University.

RUTLAND, C. J. & FERZIGER, J. 1989 Interaction of a vortex and a premixed flame. *AIAA Paper* 89-0127.

RUTLAND, C. & TROUVÉ, A. 1990 Premixed flame simulation for non-unity Lewis number. *Proc. Summer Program of the Center for Turbulence Research, Stanford University.*

SATO, J. 1982 Effects of Lewis number on extinction behavior of premixed flames in a stagnation flow. *Nineteenth Symp. (Intl) on Combustion*, p. 1541. The Combustion Institute.

SHEPHERD, I., CHENG, R. & GOIX, P. 1989 A tomographic study of premixed turbulent stagnation point flames. *Western States Section of the Combustion Institute, Livermore CA, October 23–24.*

WILLIAMS, F. A. 1985 In *Combustion Theory* (2nd ed). Benjamin Cummings.

WRAY, A. 1990 Minimal storage time-advancement schemes for spectral methods. *J. Comput. Phys.* (submitted).

ZELDOVICH, Y., BARENBLATT, G., LIBROVICH, C. & MAKHVILADZE, G. 1980 In *The Mathematical Theory of Combustion and Explosions*, p. 307. Plenum.